THE JOURNAL OF BIOLOGICAL CHEMISTRY VOL. 291, NO. 13, pp. 6895–6911, March 25, 2016

Group X Secreted Phospholipase A_2 Releases ω3 Polyunsaturated Fatty Acids, Suppresses Colitis, and Promotes Sperm Fertility*

Received for publication, January 14, 2016, and in revised form, January 27, 2016 Published, JBC Papers in Press, January 31, 2016, DOI 10.1074/jbc.M116.715672

Remi Murase[‡§1], Hiroyasu Sato[‡1], Kei Yamamoto[‡¶1], Ayako Ushida[‡‖], Yasumasa Nishito[**], Kazutaka Ikeda[‡‡], Tetsuyuki Kobayashi[‖], Toshinori Yamamoto[§], Yoshitaka Taketomi[‡], and Makoto Murakami[‡§§2]

From the [‡]Lipid Metabolism Project and [**]Core Technology and Research Center, Tokyo Metropolitan Institute of Medical Science, Tokyo 156-8506, Japan, [§]School of Pharmacy, Showa University, Tokyo 142-8555, Japan, [‖]Department of Biology, Faculty of Science, Ochanomizu University, Tokyo 112-8610, Japan, [‡‡]Laboratory for Metabolomics, RIKEN Center for Integrative Medical Sciences, Yokohama 230-0045, Japan, and [¶]PRIME and [§§]AMED-CREST, Japan Agency for Medical Research and Development, Tokyo 100-0004, Japan

Within the secreted phospholipase A_2 ($sPLA_2$) family, group X $sPLA_2$ ($sPLA_2$-X) has the highest capacity to hydrolyze cellular membranes and has long been thought to promote inflammation by releasing arachidonic acid, a precursor of pro-inflammatory eicosanoids. Unexpectedly, we found that transgenic mice globally overexpressing human $sPLA_2$-X (*PLA2G10*-Tg) displayed striking immunosuppressive and lean phenotypes with lymphopenia and increased M2-like macrophages, accompanied by marked elevation of free ω3 polyunsaturated fatty acids (PUFAs) and their metabolites. Studies using *Pla2g10*-deficient mice revealed that endogenous $sPLA_2$-X, which is highly expressed in the colon epithelium and spermatozoa, mobilized ω3 PUFAs or their metabolites to protect against dextran sulfate-induced colitis and to promote fertilization, respectively. In colitis, $sPLA_2$-X deficiency increased colorectal expression of Th17 cytokines, and ω3 PUFAs attenuated their production by lamina propria cells partly through the fatty acid receptor GPR120. In comparison, cytosolic phospholipase A_2 ($cPLA_2\alpha$) protects from colitis by mobilizing ω6 arachidonic acid metabolites, including prostaglandin E_2. Thus, our results underscore a previously unrecognized role of $sPLA_2$-X as an ω3 PUFA mobilizer *in vivo*, segregated mobilization of ω3 and ω6 PUFA metabolites by $sPLA_2$-X and $cPLA_2\alpha$, respectively, in protection against colitis, and the novel role of a particular $sPLA_2$-X-driven PUFA in fertilization.

Among the phospholipase A_2 (PLA_2)[3] family, which hydrolyzes the *sn*-2 position of phospholipids to yield fatty acids and lysophospholipids, secreted PLA_2 ($sPLA_2$) enzymes comprise the largest subgroup (1). Along with the central dogma that ω6 arachidonic acid (AA; C20:4) released by PLA_2 is converted to pro-inflammatory eicosanoids, $sPLA_2$s have long been implicated in inflammation (1). However, recent studies using $sPLA_2$ transgenic (Tg) or knock-out (KO) mice have revealed more diverse roles of $sPLA_2$s in various events through eicosanoid-dependent or -independent mechanisms in response to given microenvironmental cues (2–8). Individual $sPLA_2$s exhibit distinct tissue or cellular distributions and substrate phospholipid selectivity (in terms of polar head and *sn*-2 fatty acyl groups), which underlies their non-redundant, tissue-specific functions (9, 10).

Accumulating evidence suggests that $sPLA_2$s, while promoting inflammation, also play anti-inflammatory roles in certain situations (9, 10). $sPLA_2$-IIA protects against sepsis or pneumonia by eliminating bacteria as a "bactericidal" $sPLA_2$ (11), although it also acts as an "inflammatory" $sPLA_2$ that amplifies inflammation by hydrolyzing extracellular mitochondrial membranes (7). $sPLA_2$-V, a "Th2-prone" or "metabolic" $sPLA_2$ that is induced by Th2 cytokines or obesity-associated stress, promotes M2 polarization of macrophages partly by altering the balance between unsaturated and saturated fatty acids or by promoting phagocytic clearance of harmful materials, thereby attenuating infection, arthritis, and obesity (8, 12–15). $sPLA_2$-IID, a "resolving" $sPLA_2$ that is expressed in lymphatic dendritic cells, attenuates contact dermatitis by mobilizing ω3 polyunsaturated fatty acid (PUFA)-derived pro-resolving lipid mediators such as docosahexaenoic acid (DHA; C22:6)-derived resolvin D1 (RvD1) (5).

Among the $sPLA_2$ isoforms, group X $sPLA_2$ ($sPLA_2$-X) has the highest ability to hydrolyze phosphatidylcholine (PC), a major phospholipid in the outer leaflet of the plasma membrane (16–18). Because of this property, most previous studies have postulated that $sPLA_2$-X promotes inflammation by driv-

* This work was supported by Grants-in aid for Scientific Research from the Ministry of Education, Culture, Sports, Science and Technology of Japan 15K14957 and 15H05905 (to M. M.), 15K07959 and 25860059 (to H. S.), 23591665 and 26461671 (to K. Y.), and 24117724 and 25460087 (to Y. T.) and by PRIME (to K. Y.) and AMED-CREST (to M. M.), Japan Agency for Medical Research and Development. The authors declare that they have no conflicts of interest with the contents of this article.

[1] These authors equally contributed to this work.

[2] To whom correspondence should be addressed: Tokyo Metropolitan Institute of Medical Science, 2-1-6 Kamikitazawa, Setagaya-ku, Tokyo 156-8506, Japan. Tel.: 03-5316-3228; Fax: 03-5316-3125; E-mail: murakami-mk@igakuken.or.jp.

[3] The abbreviations used are: PLA_2, phospholipase A_2; AA, arachidonic acid; BM, bone marrow; DSS, dextran sodium sulfate; DHA, docosahexaenoic acid; DPA, docosapentaenoic acid; EPA, eicosapentaenoic acid; GI, gastrointestinal; 12-HHT, 12(*S*)-hydroxyheptadecatrienoic acid; IBD, inflammatory bowel disease; IEC, intestinal epithelial cell; LPC, lysophosphatidylcholine; LPL, lamina propria lymphocyte; PC, phosphatidylcholine; $sPLA_2$, secreted PLA_2; $sPLA_2$-X, group X $sPLA_2$; PG, prostaglandin; PE, phycoerythrin; $cPLA_2\alpha$, cytosolic phospholipase A_2; X-Tg, *PLA2G10*$^{tg/+}$.

ing AA metabolism. Indeed, mice deficient in sPLA$_2$-X (*Pla2g10*$^{-/-}$) are refractory to pulmonary and cardiovascular disorders in association with reduced eicosanoid levels (2, 19–22). In contrast, overexpression of sPLA$_2$-X in cultured macrophages elicits anti-inflammatory responses (23). Furthermore, adoptive transfer of *Pla2g10*$^{-/-}$ bone marrow (BM) cells into LDL receptor-null (*Ldlr*$^{-/-}$) mice exacerbates whereas that of human *PLA2G10*-Tg (*PLA2G10*$^{tg/+}$) BM cells ameliorates atherosclerosis and associated Th1 immunity (24). These observations suggest that sPLA$_2$-X also has anti-inflammatory roles. Moreover, lipidomics studies of sPLA$_2$-X-treated cells or lipoproteins *in vitro* have demonstrated the release of ω3 PUFAs in addition to ω6 AA (25, 26). However, the ability of sPLA$_2$-X to release ω3 PUFAs and the resulting physiological outcomes have not been investigated *in vivo*. Here, we show that sPLA$_2$-X releases ω3 PUFAs *in vivo*, thereby suppressing colitis and facilitating fertility in the respective tissues where it is highly expressed.

Experimental Procedures

Mice—Pla2g2d$^{-/-}$, *Pla2g2e*$^{-/-}$, *Pla2g2f*$^{-/-}$, *Pla2g3*$^{-/-}$, *Pla2g4a*$^{-/-}$, *Pla2g5*$^{-/-}$, *Pla2g6*$^{-/-}$, *Pla2g10*$^{-/-}$, *Ptges*$^{-/-}$, and *PLA2G10*$^{tg/+}$ mice were described previously (4–6, 8, 22, 27–30). C57BL/6 mice were obtained from SLC Japan (Shizuoka, Japan). All mice were housed in climate-controlled (23 °C) specific pathogen-free facilities with a 12-h light/dark cycle, with free access to standard diet CE2 (CLEA Japan) and water. All procedures involving animals were approved by the Institutional Animal Care and Use Committees of the Tokyo Metropolitan Institute of Medical Science, in accordance with the Standards Relating to the Care and Management of Experimental Animals in Japan.

Histology and Immunohistochemistry—Formalin-fixed tissues were embedded in paraffin, sectioned, mounted on glass slides, deparaffinized in xylene, and rehydrated in ethanol with increasing concentrations of water. The tissue sections (4 μm thick) were incubated with Target Retrieval Solution (Dako, Glostrup, Denmark) as required, incubated for 10 min with 3% (v/v) H_2O_2, washed three times with phosphate-buffered saline (PBS) for 5 min each, incubated with 5% (w/v) skim milk in PBS for 30 min, washed three times with PBS for 5 min each, and incubated with rabbit antiserum for mouse sPLA$_2$-X at 1:500 dilution in PBS overnight at 4 °C. The sections were then treated with a CSA system staining kit (Dako) with diaminobenzidine substrate, followed by counterstaining with hematoxylin and eosin.

Quantitative RT-PCR—Total RNA was extracted from tissues or cells using TRIzol reagent (Invitrogen). First-strand cDNA synthesis was performed using a high capacity cDNA reverse transcriptase kit (Applied Biosystems, Foster City, CA). PCR was carried out using Power SYBR Green or TaqMan gene expression assay (Applied Biosystems) on the ABI7700 real time PCR system (Applied Biosystems), as described previously (4–6, 8). The probe/primer sets used are listed in Table 1. *Gapdh* (4352339E; Applied Biosystems) was used as an internal control.

Preparation of Macrophages—Preparation of resident and thioglycolate-induced mouse peritoneal macrophages was described previously (30). Mouse BM cells were cultured in α-minimal essential medium (Wako, Osaka, Japan) containing 10% (v/v) fetal bovine serum (FBS; Invitrogen), 100 units/ml penicillin, and 100 μg/ml streptomycin supplemented with 100 ng/ml M-CSF (Leukoprol; Kyowa Kirin, Tokyo, Japan) to obtain BM-derived macrophages, as described previously (8). These cells were cultured for 8 h in serum-free medium and then for 24 h in culture medium supplemented with 100 ng/ml lipopolysaccharide (LPS, *Escherichia coli* O111:B4) (Sigma) plus 10 ng/ml mouse interferon (IFN)-γ (PeproTech, Rocky Hill, NJ).

TABLE 1
PCR primers used in this study
Accession numbers for TaqMan probes (Applied Biosystems) are indicated.

Name	Assay no.
Pla2g4a	Mm00447040_m1
Pla2g6	Mm00479527_m1
Pla2g1b	Mm00478249_m1
Pla2g2d	Mm00478250_m1
Pla2g2e	Mm00478870_m1
Pla2g2f	Mm00478872_m1
Pla2g5	Mm00448162_m1
Pla2g10	Mm00449532_m1
Pla2g3	Mm01191142_m1
Pla2g12a	Mm00458226_m1
Cd68	Mm03047340_m1
Arg1	Mm00475988_m1
Mrc1	Mm00485148_m1
Nos2	Mm00440502_m1
Il1b	Mm00434228_m1
Il6	Mm00446190_m1
Il17a	Mm00439618_m1
Il22	Mm00444241_m1
Tnf	Mm00443258_m1
Reg3g	Mm01181783_g1
Cd4	Mm00442754_m1
Cd8a	Mm01182107_g1
Epcam	Mm00493214_m1

Flow Cytometry—Mouse tissues were excised, minced in Hanks' solution (Nissui Pharmaceutical, Tokyo, Japan) with 2% (v/v) heat-inactivated FBS and 0.05% (w/v) sodium azide (Nacalai Tesque, Kyoto, Japan), and incubated with 400 units/ml collagenase type II (Worthington) with shaking for 30 min at 37 °C. After adding 10 mM EDTA, the suspensions were passed through cell strainer 70-μm nylon (BD Biosciences) and then centrifuged at 300 × *g* for 5 min at 4 °C. Except for analysis of the erythrocyte lineage, splenocytes or thymocytes were treated for 2 min on ice with 10 mM Tris-HCl (pH 7.0) containing 0.84% (w/v) ammonium chloride to lyse red cells, centrifuged, and suspended in Hanks' solution. For flow cytometry, the cells were subjected to blocking with mouse Block™ (BD Biosciences), incubated with phycoerythrin (PE)-conjugated anti-mouse CD11c (N418; eBioscience, San Diego, CA), PE-labeled anti-mouse CD11b (M1/70; BD Biosciences), fluorescein isothiocyanate (FITC)-labeled anti-mouse CD3ϵ (145-2C11; eBioscience), Alexa Fluor 647-labeled anti-mouse CD45R/B220 (RA3–6B2; BD Biosciences), PE-labeled anti-mouse CD4 (GK1.5; eBiosciences), Alexa 647-labeled anti-mouse CD8α (53–6.7; BioLegend, San Diego, CA), PE-labeled anti-mouse CD71 (RI7217; BioLegend), allophycocyanin (APC)-labeled TER119 (TER-119; BioLegend), or isotype control antibody (BioLegend), and analyzed by flow cytometry with a FACSAria III (BD Biosciences) and FlowJo (Tree Star, Ashland, OR) soft-

ware. Circulating blood cells were analyzed by the clinical blood cell analyzer Vetscan HMII (Abaxis, Union, CA).

Microarray—Total RNA was purified using the RNeasy mini kit (Qiagen, Venlo, Netherlands). Microarray analysis was carried out according to the manufacturer's protocol (Agilent Technologies, Santa Clara, CA), as described previously (6, 8). In brief, the quality of RNA was assessed with a 2100 Bioanalyzer. cRNA targets were synthesized with a low input QuickAmp labeling kit. Samples were hybridized to the Whole Mouse Genome microarray kit (4x44K), washed, and then scanned using a SureScan Microarray Scanner. Microarray data were analyzed with Feature Extraction software and then imported into GeneSpring GX software. Probes were normalized by quantile normalization among all microarray data. The GEO accession numbers for the microarrays are GSE77336 and GSE77144.

CT Analysis—Mice were anesthetized with Nembutal (0.5 mg/g body weight) (Dainippon Sumitomo Pharmaceutical, Osaka, Japan), and their adiposity was analyzed using the micro-CT system Latheta LCT-100 (Aloka, Tokyo, Japan), as described previously (8).

Measurement of Serum Immunoglobulin (Ig) Levels—Serum titers of IgM, IgG$_1$, IgG$_2$, and IgE were determined by a mouse IgX ELISA quantification kit (Bethyl Laboratories, Montgomery, TX).

Dextran Sodium Sulfate (DSS)-induced Colitis—DSS of average molecular weight 36,000–50,000 (MP Biomedicals, Solon, OH) was orally applied to 8-week-old male mice at a concentration of 1–3% (w/v) in drinking water. Changes in body weight were calculated every day. To assess the extent of colitis, body weight, stool consistency, and occult blood in the stool were monitored daily (31). Diarrhea was scored as follows: 0, normal; 2, loose stools; 4, watery diarrhea. Hemoccult was scored as follows: 0, normal; 2, hemoccult positive; 4, gross bleeding. On the last day of the experiments, blood was collected for determination of hematocrit using a Vetscan HMII; the colon was taken for histological examination, and the spleen was weighed and subjected to flow cytometry. As required for experiments, 2.5 μM eicosapentaenoic acid (EPA; C20:5) and 5 μM DHA (both from Cayman Chemicals, Ann Arbor, MI) in 200 μl of saline were intrarectally injected into mice every day during the period of DSS treatment.

Adoptive Transfer of BM Cells—Male *Pla2g10*$^{+/+}$ or *Pla2g10*$^{-/-}$ mice (8-week-old) were used as donors and recipients. Recipients were irradiated with 10.4 gray (M-150WE; Softex, Kanagawa, Japan) and then injected with 10^7 BM cells from donors. After 12 weeks, the recipient mice were subjected to DSS-induced colitis.

Separation of Intestinal Epithelial and Non-epithelial Cells—The large intestine was removed, opened longitudinally, washed with PBS, and incubated with PBS contaning 5 mM EDTA with shaking for 30 min at 37 °C. The tissue was separated into intestinal epithelial cells (IECs; leaflets of the epithelium) and non-IECs under a stereomicroscope, and the cells were washed with PBS before use.

Preparation of Colorectal Lamina Propria Lymphocytes (LPLs)—LPLs were prepared from C57BL/6 mice treated with 3% DSS for 7 days. Briefly, the colon (1 cm in length) was incubated with 5 mM EDTA in PBS for 20 min at 37 °C, washed twice with PBS, minced, and incubated with 20 mg/ml collagenase type 4 (Worthington) plus 0.1 mg/ml DNase (Sigma) in RPMI 1640 medium (Sigma) for 50 min at 37 °C. After filtration through a nylon mesh, floating cells were suspended in 40% Percoll (Sigma), applied onto 75% Percoll, and centrifuged at 1,000 × *g* for 20 min at room temperature. The boundary cells (LPLs) were collected, adjusted at 2×10^6 cells/ml in RPMI 1640 medium containing 10% FBS in a U-shaped 96-well plate (100 μl/well), and then cultured for 48 h to assess the release of cytokines using enzyme immunoassay kits for IL-17A (eBioscience) and IL-22 (Biolegend). As required for experiments, the cells were cultured with 1–10 μM lipids (Cayman Chemicals) or 10 μM GSK137647, a GPR120 agonist (Tocris Bioscience, Bristol, UK).

Sperm Fertility—Analyses of spermatozoa were carried out as described previously (3). Briefly, female mice (10 weeks old) were injected intraperitoneally with 7.5 IU pregnant mare serum gonadotropin (Asuka Pharmacy, Tokyo, Japan) followed 48 h later with 7.5 IU human chorionic gonadotropin (Asuka Pharmacy). After 13 h, the oocyte cumulus complexes from the oviduct were placed in 100 μl of HTF medium (ARK Resource, Kumamoto, Japan) in a 60-mm culture dish, and droplets were covered by embryo-tested mineral oil (Nakalai Tesque). Spermatozoa collected from the cauda epididymidis from male mice (8 weeks old) were allowed to swim into 50 μl of HTF medium, aspirated, incubated in 200 μl of HTF medium for 60 min at 37 °C to permit capacitation, diluted, and added to the oocyte droplets to achieve a concentration of 200 spermatozoa/μl. After incubation for 6 h at 37 °C, the oocytes were washed and cultured for 24 h. Fertilization was evaluated by the presence of a second polar body and two pronuclei. As required for experiments, lipids (1 μM) were added to the *in vitro* fertilization assay.

Electrospray Ionization-Mass Spectrometry (ESI-MS)—All procedures were performed as described previously (4, 5). In brief, tissues were soaked in 10 volumes of methanol and homogenized with a Polytron homogenizer. After overnight incubation at −20 °C, H_2O was added to the mixture to give a final methanol concentration of 10% (v/v). As internal standards for determination of recovery, 1 ng of d_5-labeled EPA, d_4-labeled leukotriene B_4, d_4-labeled prostaglandin (PG) E_2, and d_8-labeled 15-hydroxyeicosatetraenoic acid (Cayman Chemicals) were added to the samples. The oxygenated lipids in the supernatant were extracted using Sep-Pak C18 cartridges (Waters, Milford, MA), where the samples in 10% methanol were applied to the cartridges, washed with 10 ml of hexane, eluted with 3 ml of methyl formate, dried up under N_2 gas, and dissolved in 60% methanol. The analysis of PUFAs and their metabolites was performed using a 4000Q-TRAP quadrupole-linear ion trap hybrid mass spectrometer (AB Sciex, Framingham, MA) with liquid chromatography (LC) (LC-20AP; Shimadzu, Kyoto, Japan) combined with an HTC PAL autosampler (CTC Analytics, Zwingen, Switzerland). The sample was applied to the Develosil C30-UG column (1 × 150 mm inner diameter, 3 μm particles) (Nomura Chemical, Aichi, Japan) coupled for ESI-MS/MS. The samples injected by the autosampler (10 μl) were directly introduced and separated by

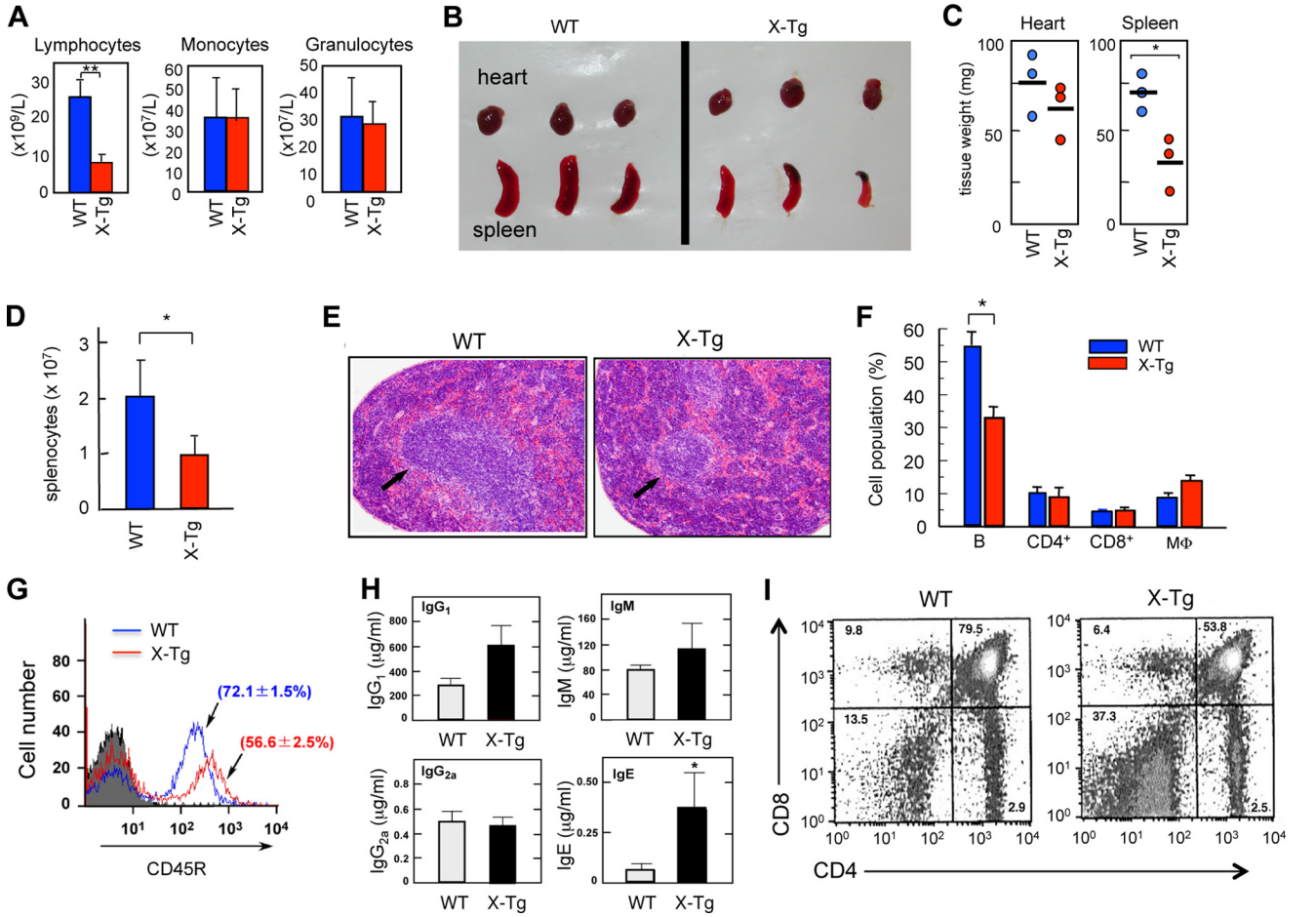

FIGURE 1. ***PLA2G10$^{tg/+}$* mice display lymphopenia.** *A*, circulating leukocyte counts in 8-week-old male WT and *PLA2G10$^{tg/+}$* (*X-Tg*) mice ($n = 4$). *B* and *C*, photos (*B*) and weights (*C*) of heart and spleen from WT and X-Tg mice ($n = 3$). *D*, total counts of splenocytes in WT and X-Tg mice ($n = 3$). *E*, hematoxylin-eosin staining of the spleen of 8-week-old WT and *PLA2G10$^{tg/+}$* mice. *Arrows* indicate white pulps. *F*, immune cell population of splenocytes in WT and X-Tg mice as revealed by FACS analysis ($n = 3$). *G*, FACS profile of B cells for CD45R expression in WT and X-Tg mice. Values indicates % cell population ($n = 3$). *H*, serum Ig levels in WT and X-Tg mice ($n = 4$). *I*, FACS profiles of thymocytes for CD4 and CD8 expression in 1-year-old WT and X-Tg mice. Mean ± S.D., *, $p < 0.05$, and **, $p < 0.01$.

a step gradient with mobile phase A (water containing 0.1% acetic acid) and mobile phase B (acetonitrile: methanol = 4: 1; v/v) at a flow rate of 50 μl/min and a column temperature of 45 °C.

For detection of phospholipids, tissues were soaked in 10 volumes of 20 mM Tris-HCl (pH 7.4) and then homogenized with a Polytron homogenizer. Phospholipids were extracted and subjected to ESI-MS using a 4000Q-TRAP and LC-20AP with Develosil C30-UG column, as described previously (4). As an internal standard, 1 nmol of LPC(17:0) (Avanti Polar Lipids, Alabaster, AL) was added to each sample. The samples were separated by a step gradient with mobile phase A (acetonitrile/methanol/water = 1:1:1 (v/v/v) containing 5 μM phosphoric acid and 1 mM ammonium formate) and mobile phase B (2-propanol containing 5 μM phosphoric acid and 1 mM ammonium formate) at a flow rate of 80 μl/min at 50 °C.

Identification was conducted using multiple reaction monitoring transition and retention times, and quantification was performed based on peak area of the multiple reaction monitoring transition and the calibration curve obtained with an authentic standard for each lipid (Avanti Polar Lipids and Cayman Chemicals).

Statistical Analysis—Data are expressed as mean ± S.E. or S.D. Statistical significance between groups was evaluated by two-tailed Student's *t* test or one-way analysis of variance at a significance level of $p < 0.05$.

Results

Immunosuppressive Phenotypes in PLA2G10$^{tg/+}$ Mice—Although our analysis of *PLA2G10$^{tg/+}$* mice was underway (4), we noticed that *PLA2G10$^{tg/+}$* mice had fewer circulating lymphocytes than did wild-type (WT) mice (Fig. 1*A*), contrary to our prediction that sPLA$_2$-X overexpression would increase immune cells through its proposed pro-inflammatory action. Consistent with the lymphopenia, the weight of the spleen relative to that of the heart was significantly lower (Fig. 1, *B* and *C*); the number of splenocytes was ~50% lower (Fig. 1*D*), and the splenic white pulps appeared smaller (Fig. 1*E*) in *PLA2G10$^{tg/+}$* mice than in WT mice. Although the proportions of splenic CD4$^+$ or CD8$^+$ T cells and CD11b$^+$ monocytes/macrophages were unchanged, the proportion of CD45R$^+$ B cells was lower in *PLA2G10$^{tg/+}$* mice than in WT mice (Fig. 1, *F* and *G*). As the absolute number of splenocytes was reduced in *PLA2G10$^{tg/+}$* mice, the total counts of splenic T cells and monocytes/macro-

TABLE 2

Microarray gene profiling of the thymus of *PLA2G10$^{tg/+}$* mice *versus* WT mice

Total RNAs were isolated from the thymus of *PLA2G10$^{tg/+}$* and littermate WT mice at 6 months. Equal amounts of total RNA (pooled from four mice for each genotype) were subjected to two-color gene expression microarray analysis. Data were processed using the Feature Extraction software from Agilent. Representative genes that showed decreased expression in transgenic (Tg) mice relative to WT mice are listed.

Gene name	Accession no.	Tg/WT	Description
Klf2	NM_008452	0.403	Kruppel-like factor 2
Cd8a	AK088128	0.481	CD8 antigen, α-chain
Ccr9	NM_009913	0.526	Chemokine (C-C motif) receptor 9
Dynll1	NM_019682	0.532	Dynein light chain LC8-type 1
Ets2	NM_011809	0.544	E26 avian leukemia oncogene 2, 3′ domain
Wdr78	NM_146254	0.584	WD repeat domain 78
Rorc	NM_011281	0.623	RAR-related orphan receptor γ
Traf4	NM_009423	0.623	TNF receptor-associated factor 4
Rgs14	NM_016758	0.642	Regulator of G-protein signaling 14
Kpna2	NM_010655	0.643	Karyopherin (importin) α2
Phlda1	NM_009344	0.657	Pleckstrin homology-like domain family A member 1
Soat1	NM_009230	0.663	Sterol *O*-acyltransferase 1
Cpne1	NM_170588	0.666	CopineI (Cpne1), transcript variant 1
Nup35	NM_027091	0.671	Nucleoporin 35
Tdrd5	XM_129603	0.673	Tudor domain containing 5
Phf23	NM_030064	0.674	PHD finger protein 23
Bysl	NM_016859	0.679	Bystin-like
Jmjd3	NM_001017426	0.686	Jumonji domain containing 3
Klf3	NM_008453	0.690	Kruppel-like factor 3 (basic)
Srm	NM_009272	0.693	Spermidine synthase
Sla2	BC052655	0.693	Src-like adaptor 2
Obfc2a	BC095967	0.705	Oligonucleotide/oligosaccharide-binding fold containing 2A
Hsp110	NM_013559	0.706	Heat shock protein 110
Zcchc7	NM_177027	0.709	Zinc finger, CCHC domain containing 7
Ppp1r10	NM_175934	0.711	Protein phosphatase 1, regulatory subunit 10
Hspa4	NM_008300	0.729	Heat shock protein 4
Lxn	NM_016753	0.734	Latexin (Lxn)
Dhrs3	NM_011303	0.736	Dehydrogenase/reductase (SDR family) member 3

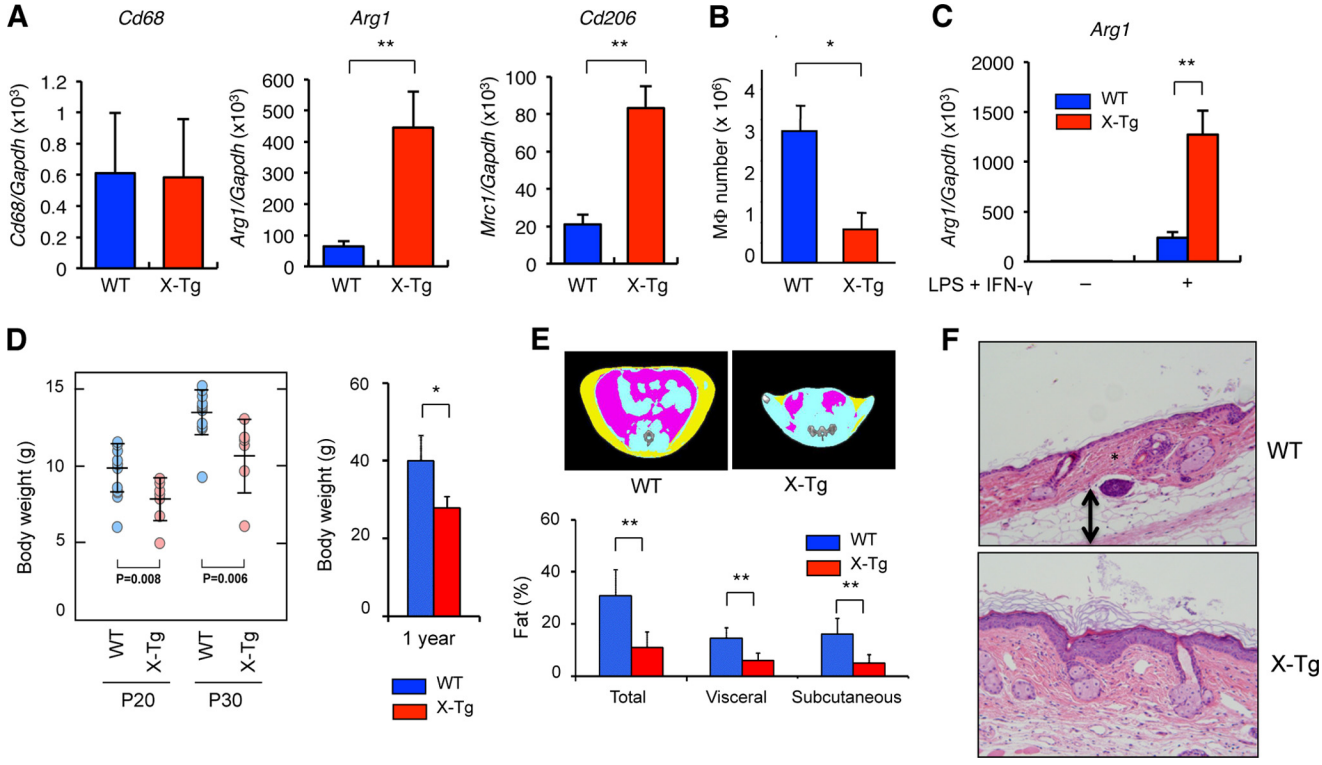

FIGURE 2. **Immunosuppressive and lean phenotypes in *PLA2G10$^{tg/+}$* mice.** *A*, expression of M1 or M2 macrophage markers in resident peritoneal macrophages from WT and X-Tg mice ($n = 6$). *B*, counts of thioglycollate-induced macrophages in the peritoneal cavity of WT and X-Tg mice ($n = 4$). *C*, expression of the M2 macrophage marker *Arg1* in BM-derived macrophages from WT or X-Tg mice with or without stimulation for 24 h with LPS + IFN-γ ($n = 4$). *D*, body weights of WT and X-Tg mice at indicated ages ($n = 5$). *E*, CT scanning of visceral (*red*) and subcutaneous (*yellow*) fat (*upper panel*) and quantification of total, visceral, and subcutaneous fat (*lower panel*) in 1-year-old WT and X-Tg mice ($n = 5$). *F*, hematoxylin-eosin staining of the skin of 1-year-old WT and X-Tg mice. *Arrow* indicates subcutaneous fat. Mean ± S.E. (*A–C*) or mean ± S.D. (*D* and *E*), *, $p < 0.05$, and **, $p < 0.01$.

phages were proportionally lower in *PLA2G10$^{tg/+}$* mice than in WT mice. Furthermore, the median fluorescence intensity of CD45R on B cells was greater in *PLA2G10$^{tg/+}$* mice than in WT mice (Fig. 1*G*), indicative of altered B cell differentiation. Despite the lower proportion of B cells, serum levels of IgG_1 and IgE, but not IgM and IgG_{2a}, were higher in *PLA2G10$^{tg/+}$* mice

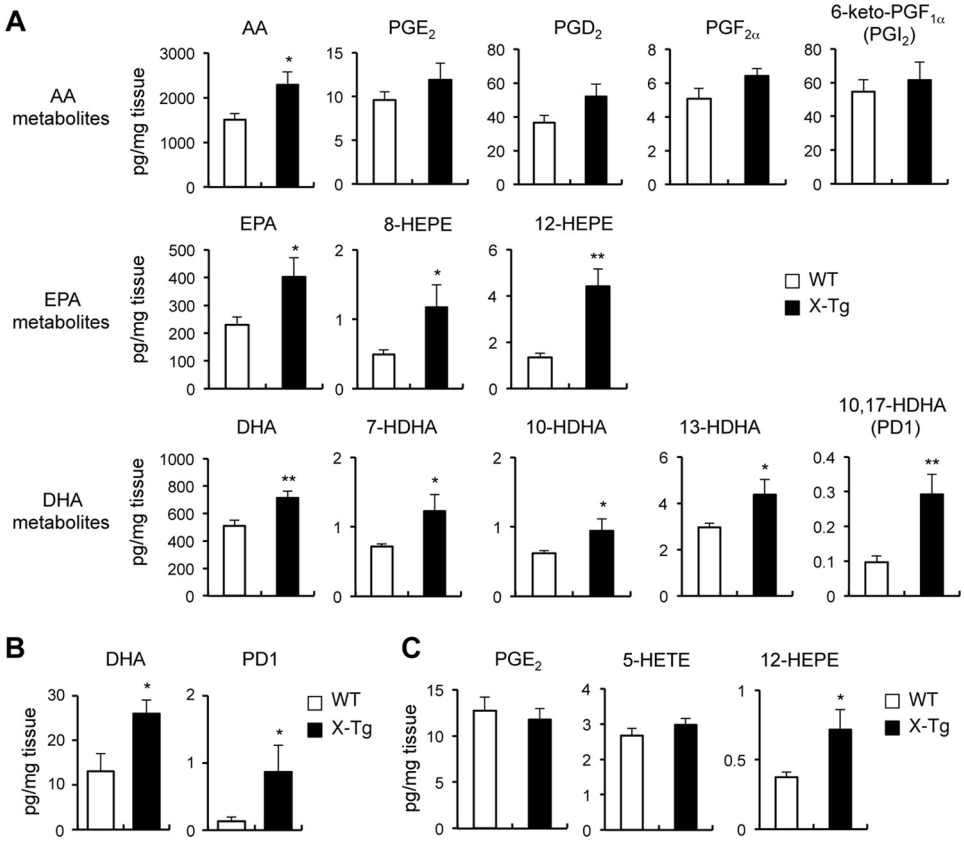

FIGURE 3. **ESI-MS profiling of PUFA metabolites in *PLA2G10*$^{tg/+}$ mice.** Lipids were extracted from spleen (*A*), skin (*B*), and colon (*C*) of WT and X-Tg mice. PUFAs and their metabolites were analyzed by ESI-MS (n = 5–9). Mean ± S.E., *, $p < 0.05$, and **, $p < 0.01$. *HEPE*, hydroxyeicosapentaenoic acid; *HETE*, 15-hydroxyeicosatetraenoic acid; *HDHA*, hydroxydocosahexaenoic acid.

than in WT mice (Fig. 1*H*), suggesting preferential skewing toward a Th2 response, which on the one hand promotes allergies and on the other hand suppresses Th1/Th17-based diseases such as arthritis, atherosclerosis, obesity, and colitis (32).

In the thymus, *PLA2G10*$^{tg/+}$ mice had fewer CD4$^+$CD8$^+$ double-positive and more CD4$^-$CD8$^-$ double-negative cells than did WT mice (Fig. 1*I*), indicating perturbed thymocyte transition from the double-negative to the double-positive stage in the thymic cortex of *PLA2G10*$^{tg/+}$ mice. In support of this, microarray gene profiling of the thymus revealed lower expression of genes crucial for differentiation, proliferation, survival, and migration of thymocytes (*e.g. Cd8a, Ccr9, Rorc, Klf2,* and *Ets2*) (33–37) in *PLA2G10*$^{tg/+}$ mice than in WT mice (Table 2).

Resident peritoneal macrophages in *PLA2G10*$^{tg/+}$ mice showed greater expression of the M2 macrophage markers *Arg1* and *Cd206* than did WT mice, although expression of the M1 macrophage marker *Cd68* was comparable in both genotypes (Fig. 2*A*). The count of thioglycolate-induced macrophages in the peritoneal cavity was lower in *PLA2G10*$^{tg/+}$ mice than in WT mice (Fig. 2*B*), suggesting a reduced ability of monocytes to migrate to sites of inflammation or to differentiate into pro-inflammatory M1-like macrophages. M-CSF-driven BM-derived macrophages from *PLA2G10*$^{tg/+}$ mice showed greater expression of the M2 marker *Arg1* than did WT mice, even when they were cultured with M1 polarizers (LPS + IFN-γ) (Fig. 2*C*).

In agreement with the view that M2 macrophages and Th2 immunity counteract metabolic diseases (8, 32), *PLA2G10*$^{tg/+}$ mice had lower body weight (Fig. 2*D*) and adiposity (Fig. 2*E*) than did WT mice throughout their life span. The subcutaneous fat layer, which was obviously present in WT mice, was scarcely seen in *PLA2G10*$^{tg/+}$ mice (Fig. 2*F*). Thus, Tg overexpression of sPLA$_2$-X facilitates M2 polarization of macrophages, which may account, at least partly, for the anti-inflammatory and lean phenotypes.

We next assessed whether the anti-inflammatory phenotypes observed in *PLA2G10*$^{tg/+}$ mice might be ascribed to the capacity of sPLA$_2$-X to alter lipid profiles *in vivo*. ESI-MS revealed that the splenic levels of AA, EPA, and DHA were significantly greater in *PLA2G10*$^{tg/+}$ mice than in WT mice (Fig. 3*A*). The levels of AA metabolites tended to be slightly higher in *PLA2G10*$^{tg/+}$ mice than in WT mice, but none of them reached statistical significance. Notably, the levels of ω3 PUFA metabolites, such as hydroxyeicosapentaenoic acids and hydroxydocosahexaenoic acids (including protectin D1 (PD1)), were significantly increased in *PLA2G10*$^{tg/+}$ mice relative to WT mice (Fig. 3*A*). The increase of ω3 PUFAs and their metabolites in *PLA2G10*$^{tg/+}$ mice was not limited to the spleen, because the skin levels of DHA and its metabolite PD1 were also higher in *PLA2G10*$^{tg/+}$ mice than in WT mice (Fig. 3*B*), although AA and its metabolite PGE$_2$ were also increased in the transgenic skin (4). In the colon, significant increases of EPA, rather than AA, metabolites were evident (Fig. 3*C*). Taken

together, these results suggest a previously unappreciated capacity of sPLA$_2$-X to mobilize ω3 PUFAs and their metabolites *in vivo*. Given the well established anti-inflammatory role of ω3 PUFAs and their metabolites (38, 39), the lipid profiles altered thus far could explain, at least in part, the immunosuppressive phenotypes in *PLA2G10*$^{tg/+}$ mice.

Exacerbation of Colitis in Pla2g10$^{-/-}$ *Mice*—Given these observations, we next searched for a particular pathophysiological condition under which endogenous sPLA$_2$-X would play an anti-inflammatory role. To this end, we focused on inflammation in the gastrointestinal (GI) tract, where endogenous sPLA$_2$-X is abundantly expressed (40, 41). Inflammatory bowel disease (IBD) is a chronic, relapsing, and remitting condition of unknown origin that exhibits various features of immunological disorders, including impaired mucosal barrier function, pronounced innate and acquired immunity, and dysregulated production of cytokines, chemokines, and lipid mediators (42–44). Both ω6 AA metabolites, such as PGE$_2$ and 12(*S*)-hydroxyheptadecatrienoic acid (12-HHT) (31, 45, 46), and ω3 PUFAs or their metabolites, such as resolvins D and E (47–49), are protective against IBD. However, the PLA$_2$ subtypes that lie upstream of the production of these lipid mediators in this disease are currently unknown.

Among the sPLA$_2$s, *Pla2g10* (X) was expressed most abundantly in C57BL/6 colon, followed in order by *Pla2g5* (V), *Pla2g2f* (IIF), *Pla2g3* (III), and *Pla2g12a* (XIIA), whereas *Pla2g1b* (IB), *Pla2g2d* (IID), and *Pla2g2e* (IIE) were detected only at trace levels (Fig. 4*A*). *Pla2g4a,* and to a lesser extent *Pla2g6* (which encode group IVA cytosolic PLA$_2$ (cPLA$_2\alpha$) and group VIA Ca^{2+}-independent PLA$_2$ (iPLA$_2\beta$), respectively), were also expressed at substantial levels in the colon. Immunohistochemistry of the colon showed that sPLA$_2$-X protein was localized in IECs and goblet cells, although its staining was absent in *Pla2g10*$^{-/-}$ mice (Fig. 4*B*). Consistently, *Pla2g10* mRNA was enriched in *Epcam*-positive IECs isolated from WT colon (Fig. 4*C*). In DSS-induced ulcerative colitis, a well known model of IBD (50), the colorectal expression of *Pla2g10* as well as *Pla2g2f, Pla2g3, Pla2g12a,* and *Pla2g6* was decreased in mice treated for 7 days with 3% DSS (Fig. 4*A*), probably due to the collapse of the mucosal epithelium or in unknown ways. The expression of *Pla2g4a* and *Pla2g5* was constant regardless of DSS challenge, suggesting that they are distributed mainly in cells other than IECs.

To assess the roles of sPLA$_2$s in IBD, we applied the DSS-induced colitis model to mice lacking individual sPLA$_2$s expressed in the colon. Notably, *Pla2g10*$^{-/-}$ mice exhibited more severe colitis than did WT mice. After a lag period of several days after exposure to 1% DSS, *Pla2g10*$^{-/-}$ mice displayed more severe body weight loss (Fig. 5*A*), fecal bleeding plus diarrhea (summarized as the clinical score) (Fig. 5*B*), and colon shortening (Fig. 5*C*) than did WT mice. Histologically, more advanced epithelial loss, crypt damage, ulceration, and submucosal infiltration of immune cells were evident in the colon of DSS-treated *Pla2g10*$^{-/-}$ mice than was the case for WT mice (Fig. 5*D*). In comparison, mice lacking other sPLA$_2$s, including *Pla2g2d*$^{-/-}$, *Pla2g2e*$^{-/-}$, *Pla2g2f*$^{-/-}$, *Pla2g3*$^{-/-}$, and *Pla2g5*$^{-/-}$ mice, showed no obvious phenotypes in this model (Fig. 5*E*).

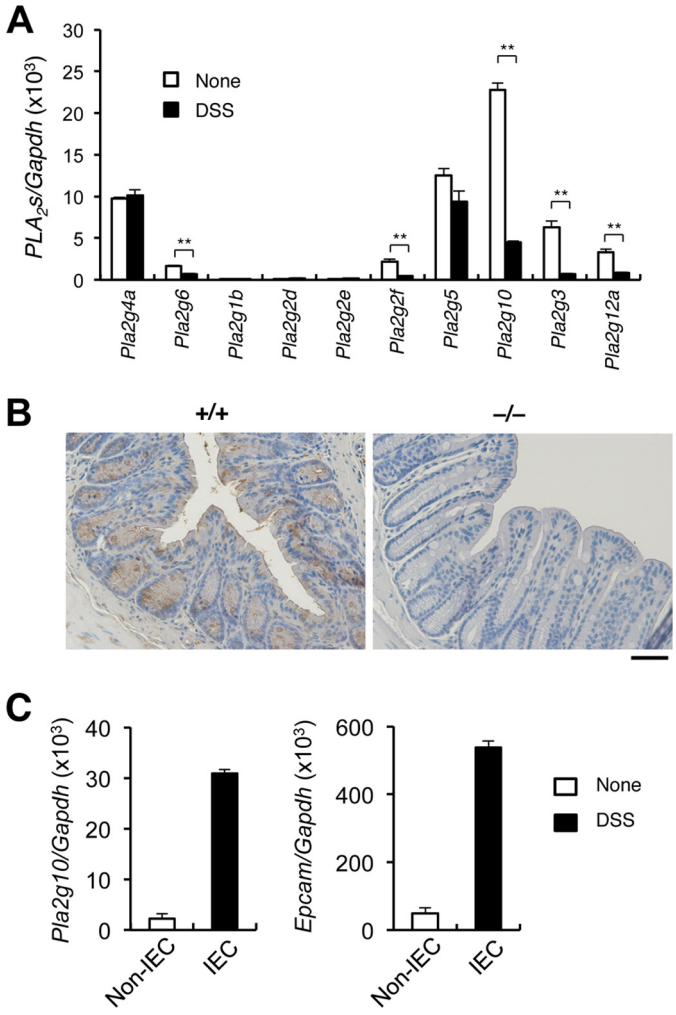

FIGURE 4. **Expression of sPLA$_2$s in C57BL/6 mouse colon.** *A,* quantitative RT-PCR of various sPLA$_2$s in WT colon with or without administration of 3% DSS for 7 days ($n = 3$). *B,* immunohistochemistry of sPLA$_2$-X in WT colon (*bar,* 50 μm). *C,* quantitative RT-PCR of *Pla2g10* in IEC and non-IEC cells in WT colon ($n = 3$). Mean ± S.E., **, $p < 0.01$.

Quantitative RT-PCR of the colon revealed that the expression levels of genes related to pro-inflammatory and Th17-related cytokines (*Il1b, Il6, Il17a, Il22,* and *Tnf*) were increased more robustly in *Pla2g10*$^{-/-}$ mice than in *Pla2g10*$^{+/+}$ mice after DSS challenge (Fig. 5*F*). Expression of *Reg3g,* which encodes an IL-22-inducible anti-bacterial protein (42, 43), as well as that of CD4$^+$ and CD8$^+$ T cell markers (*Cd4* and *Cd8a*; the latter in particular) also tended to be higher in DSS-treated *Pla2g10*$^{-/-}$ than in *Pla2g10*$^{+/+}$ mice (Fig. 5*F*). Expression of both M1 and M2 macrophage markers (*Nos2* and *Arg1*, respectively) was also greater in DSS-treated *Pla2g10*$^{-/-}$ mice than in *Pla2g10*$^{+/+}$ mice, suggesting that the absence of sPLA$_2$-X affected recruitment, rather than polarization, of macrophages in this setting. These results were further supported by microarray gene profiling, where colorectal expression of various cytokines, chemokines, macrophage markers, and other inflammatory genes was elevated in DSS-treated *Pla2g10*$^{-/-}$ mice relative to *Pla2g10*$^{+/+}$ mice (Table 3). Even in the control group, expression of the pro-inflammatory and anti-bacterial genes *S100a8* and *S100a9* was higher in *Pla2g10*$^{-/-}$ mice than in *Pla2g10*$^{+/+}$ mice, suggesting that some colorectal abnormal-

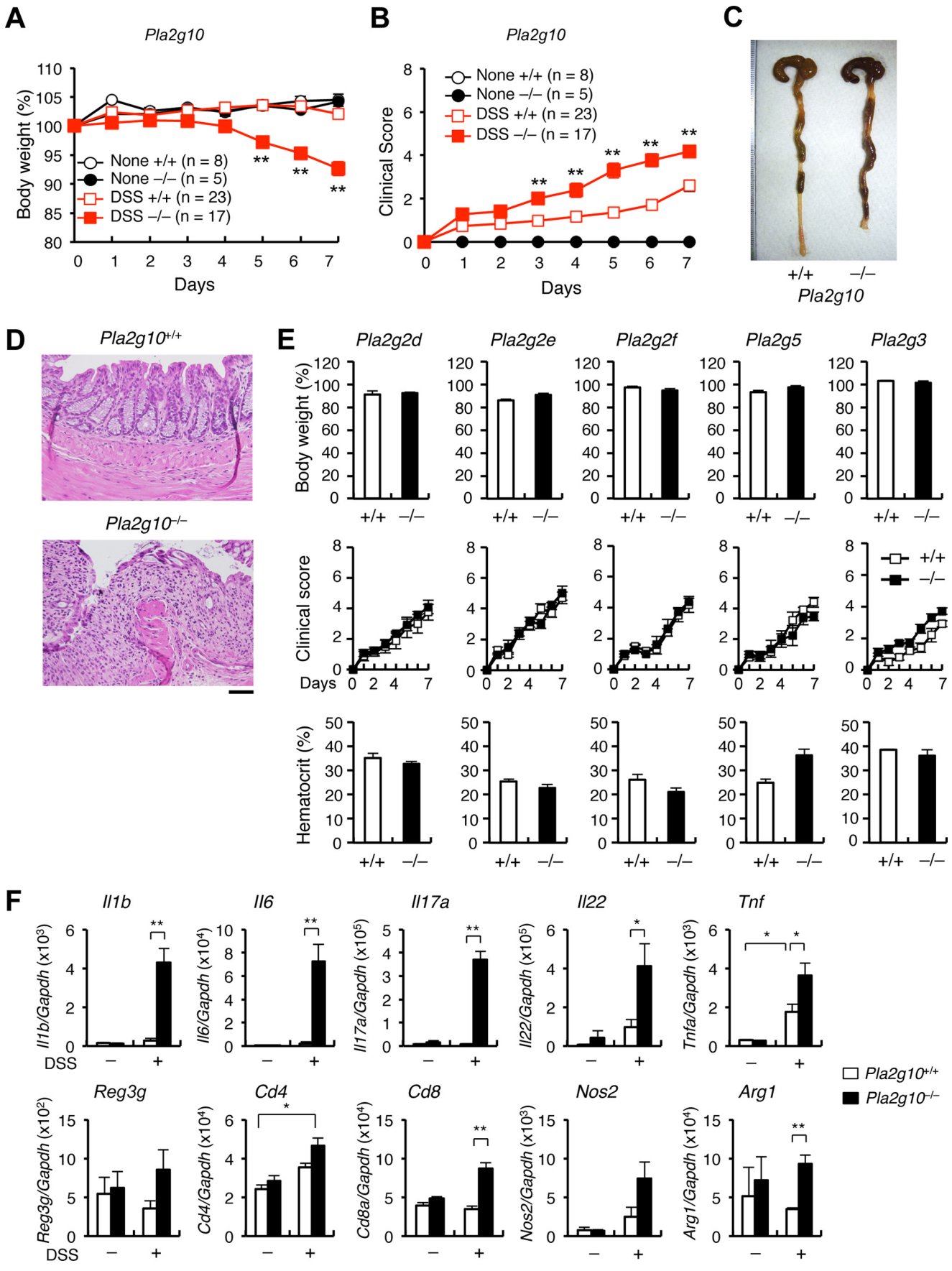
A
Pla2g10
Body weight (%)
Days
None +/+ (n = 8)
None –/– (n = 5)
DSS +/+ (n = 23)
DSS –/– (n = 17)
B
Pla2g10
Clinical Score
Days
C
+/+
–/–
Pla2g10
D
Pla2g10+/+
Pla2g10–/–
E
Pla2g2d
Pla2g2e
Pla2g2f
Pla2g5
Pla2g3
Body weight (%)
Clinical score
Days
Hematocrit (%)
F
Il1b
Il6
Il17a
Il22
Tnf
Reg3g
Cd4
Cd8
Nos2
Arg1
DSS
Pla2g10+/+
Pla2g10–/–

TABLE 3

Microarray gene profiling of the colon of *Pla2g10*$^{-/-}$ mice *versus* *Pla2g10*$^{+/+}$ mice in DSS-induced colitis

Total RNAs were isolated from the colons of *Pla2g10*$^{+/+}$ (WT) and *Pla2g10*$^{-/-}$ (KO) mice with or without 1% DSS treatment for 1 week. Equal amounts of total RNA (pooled from three mice for each genotype) were subjected to one-color gene expression microarray analysis. Data were processed using the Feature Extraction software from Agilent and analyzed using GeneSpring software. Fold changes (KO relative to WT) on the microarray are listed.

Gene name	Accession no.	DSS(−) KO/WT	DSS(+) KO/WT
Cytokines and their receptors			
Il1b	NM_008361	1.74	2.92
Il6	NM_031168	0.70	2.85
Il17a	NM_010552	0.45	2.94
Il2	NM_008366	1.07	7.12
Il7r	NM_008372	1.15	2.05
Chemokines and their receptors			
Ccl4	NM_013652	1.24	4.07
Ccl7	NM_013654	0.60	2.25
Ccr6	NM_009835	1.35	2.44
Cxcl13	NM_018866	1.21	5.49
Cxcl2	NM_009140	0.93	4.60
Macrophages			
Emr1	NM_010130	0.76	2.24
Nos2	NM_010927	0.76	2.72
Cd68	NM_009853	0.59	2.04
Arg1	NM_007482	1.00	3.36
Chi3l3	NM_009892	1.07	3.58
Inflammation-related			
S100a9	NM_001281852	3.60	5.18
S100a8	NM_013650	3.35	5.86
Ptgs2	NM_011198	1.14	2.64
Mmp3	NM_010809	0.66	2.98
Mmp9	NM_013599	0.52	3.02
Mmp10	NM_019471	0.72	3.65
Epithelial cells			
Krt78	NM_212487	0.76	0.43
Krt1	NM_008473	1.33	0.15
Defb23	NM_001037933	1.03	0.08
Defb45	NM_001037752	0.99	0.25

ities were already present in the null mice under normal housing conditions. In contrast, expression of several epithelial markers was lower in DSS-treated *Pla2g10*$^{-/-}$ than in *Pla2g10*$^{+/+}$ mice (Table 3), consistent with the increased epithelial collapse in the former.

DSS-treated *Pla2g10*$^{-/-}$ mice showed more profound splenomegaly (Fig. 6, *A* and *B*) and a decrease in hematocrit (Fig. 6*C*) relative to *Pla2g10*$^{+/+}$ mice, suggesting alternation of extramedullary erythropoiesis due to colorectal bleeding. Indeed, flow cytometry of cells in the erythrocyte lineage (in terms of CD71 and TER119 expression) revealed increased accumulation of immature erythroblasts and reticulocytes, with reciprocal decreases in mature erythrocytes, in the blood (Fig. 6, *D* and *E*) and even more profoundly in the spleen (Fig. 6, *F* and *G*) of DSS-treated *Pla2g10*$^{-/-}$ mice relative to replicate *Pla2g10*$^{+/+}$ mice. This trend was already evident, albeit modestly, even in the control group (Fig. 6, *D* and *F*). These results suggest that the transition from immature to mature erythrocytes is disturbed by *Pla2g10* deficiency, particularly under the conditions of colitis.

To evaluate the relative contribution of sPLA$_2$-X in the hematopoietic and non-hematopoietic compartments to DSS-induced colitis, BM cells from *Pla2g10*$^{+/+}$ or *Pla2g10*$^{-/-}$ mice were adoptively transferred into lethally irradiated *Pla2g10*$^{+/+}$ or *Pla2g10*$^{-/-}$ mice, which were then subjected to the colitis model (Fig. 7*A*). When the donor BM cells from *Pla2g10*$^{+/+}$ or *Pla2g10*$^{-/-}$ mice were transferred into recipient *Pla2g10*$^{+/+}$ mice (WT → WT or KO → WT), there were no differences in body weight (Fig. 7*B*) or clinical score (Fig. 7*C*) between the groups. In contrast, weight loss (Fig. 7*B*) and an increased clinical score (Fig. 7*C*) were obvious in *Pla2g10*$^{-/-}$ mice that received *Pla2g10*$^{+/+}$ BM cells (WT → KO) in comparison with WT → WT or KO → WT chimeras. When *Pla2g10*$^{-/-}$ mice were used as both donors and recipients (KO → KO), the weight loss (Fig. 7*B*) and increased clinical score (Fig. 7*C*) were similar to those in WT → KO chimeras. These results suggest that sPLA$_2$-X in non-hematopoietic cells, most likely IECs, is mainly responsible for the protection from colitis. Of note, DSS-induced splenomegaly (Fig. 7*D*) and the decrease in hematocrit (Fig. 7*E*) were significantly more severe in KO → KO chimeras than in WT → KO chimeras, implying an additional contribution of hematopoietic sPLA$_2$-X to these processes in the absence of non-hematopoietic sPLA$_2$-X.

sPLA$_2$-X Mobilizes ω3 PUFAs in Colitis—To gain insights into the mechanism underlying the anti-inflammatory action of sPLA$_2$-X in colitis, lipids extracted from colon tissues of *Pla2g10*$^{+/+}$ and *Pla2g10*$^{-/-}$ mice with or without DSS treatment were subjected to ESI-MS. We found that the colon levels of EPA, docosapentaenoic acid (DPA; C22:5), and DHA were increased in WT mice following DSS treatment, whereas these changes were not evident in *Pla2g10*$^{+/+}$ mice (Fig. 8*A*). AA also showed a similar trend but did not reach statistical significance (Fig. 8*A*). *Pla2g10* deficiency did not alter the basal levels of these PUFAs. Strikingly, the colorectal levels of AA metabolites were not affected by *Pla2g10* deficiency (Fig. 8*B*), whereas those of EPA or DHA metabolites, such as resolvins and 18-HEPE, were substantially lower in DSS-treated *Pla2g10*$^{-/-}$ mice than in *Pla2g10*$^{+/+}$ mice (Fig. 8*C*). These results, together with the results of *PLA2G10*$^{tg/+}$ mice (see above) and the reported role of ω3 PUFA metabolites in the protection against colitis (47–49), raise the possibility that the mobilization of ω3 PUFAs or their metabolites may underlie the anti-inflammatory role of sPLA$_2$-X in colitis.

When LPLs isolated from DSS-treated WT mice were incubated with PUFAs *ex vivo*, production of Th17 cytokines, IL-17A and IL-22, was partially suppressed by ω3 PUFAs (EPA, DPA and DHA) as well as by ω6 AAs, although their metabolites (resolvins and 18-HEPE) were ineffective in this assay (Fig.

FIGURE 5. **Exacerbation of DSS-induced colitis in *Pla2g10*$^{-/-}$ mice.** *A* and *B*, daily monitoring of body weight loss (*A*) and clinical score (*B*) in *Pla2g10*$^{+/+}$ and *Pla2g10*$^{-/-}$ mice (8-week-old, male) that were untreated or orally administered 1% DSS. *C* and *D*, gross appearance (*C*) and histology (*D*) of the colon in *Pla2g10*$^{+/+}$ and *Pla2g10*$^{-/-}$ mice after treatment with DSS for 7 days. *Bar*, 50 μm. *E*, DSS-induced colitis in knock-out mice for various sPLA$_2$s. *Pla2g2d*$^{-/-}$, *Pla2g2e*$^{-/-}$, *Pla2g2f*$^{-/-}$, *Pla2g5*$^{-/-}$, or *Pla2g3*$^{-/-}$ mice and their corresponding control mice were administered 1% DSS orally and evaluated for body weight on day 7 (*top*), clinical score at the indicated times (*middle*), and hematocrit on day 7 (*bottom*) ($n = 4–6$). *F*, quantitative RT-PCR of inflammation-associated genes in the colon of *Pla2g10*$^{+/+}$ and *Pla2g10*$^{-/-}$ mice after treatment with or without DSS for 7 days ($n = 5$ (without DSS) or 6 (with DSS)). Mean ± S.E., *, $p < 0.05$, and **, $p < 0.01$.

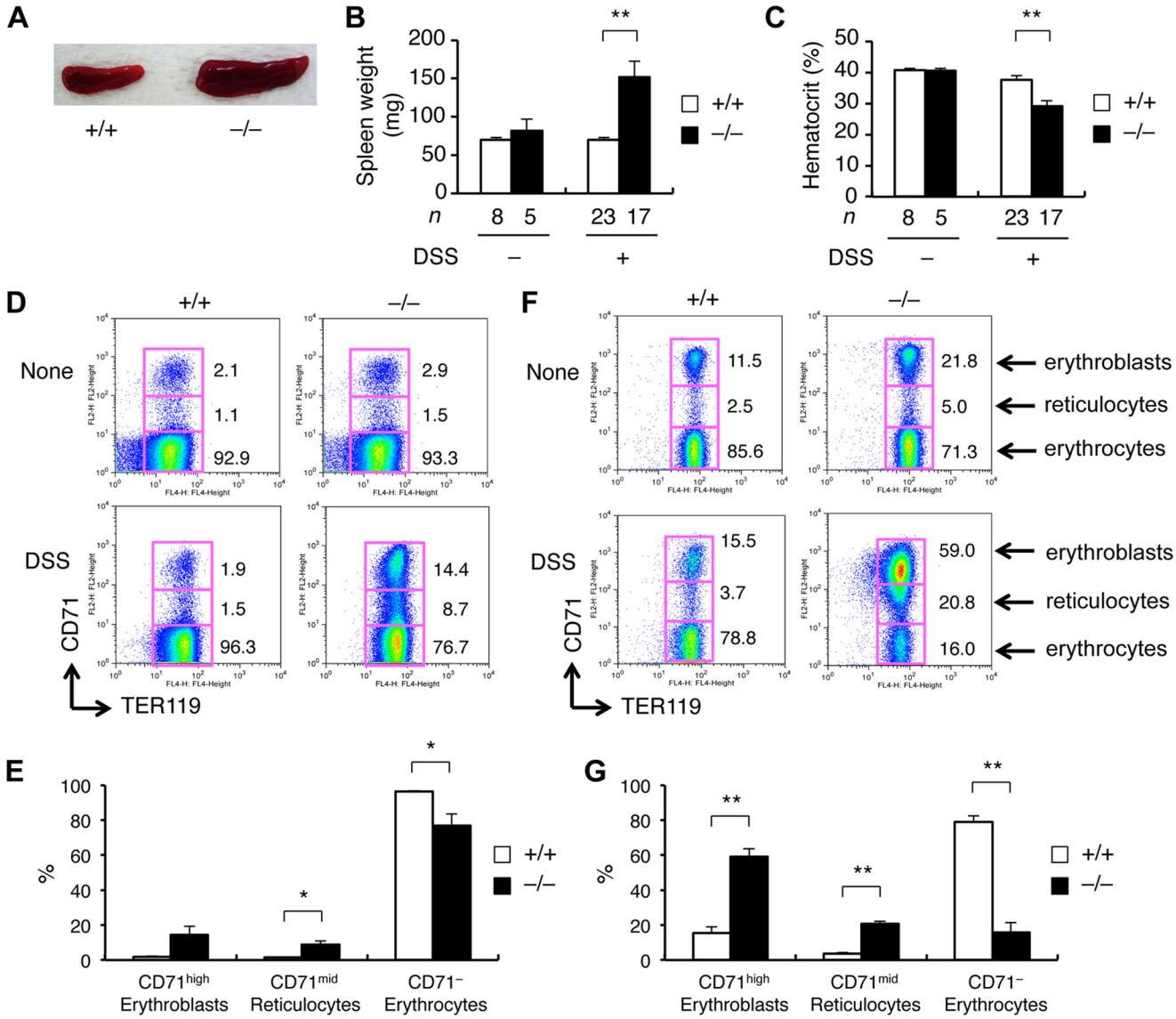

FIGURE 6. **Altered extramedullary erythropoiesis in DSS-treated *Pla2g10*$^{-/-}$ mice.** *A–C*, representative appearance of the spleen (*A*), spleen weight (*B*), and hematocrit (*C*) in *Pla2g10*$^{+/+}$ and *Pla2g10*$^{-/-}$ mice after treatment for 7 days with or without 1% DSS. *D–G*, flow cytometry of the erythrocyte lineage in the blood (*D* and *E*) and spleen (*F* and *G*) of *Pla2g10*$^{+/+}$ and *Pla2g10*$^{-/-}$ mice with or without administration of DSS for 7 days. Representative FACS profiles (*D* and *F*) and quantified results ($n = 3$) are shown. Mean ± S.E., *, $p < 0.05$, and **, $p < 0.01$.

8*D*). Because these PUFAs can act on the fatty acid receptor GPR120 or GPR40 (51), we tested the effect of GSK137647, a GPR120-selective agonist, on cytokine production by LPLs. The release of IL-17A and IL-22 was suppressed by GSK137647 as efficiently as DHA (Fig. 8*E*), indicating that PUFAs may act, at least in part, on GPR120 on LPLs, thereby partially dampening the Th17 cytokine production. Moreover, daily intrarectal injection of ω3 PUFAs (a mixture of EPA and DHA) into *Pla2g10*$^{-/-}$ mice prevented DSS-induced body weight loss (Fig. 8*F*). Overall, these results further support the notion that sPLA$_2$-X prevents colitis by releasing ω3 PUFAs. Nonetheless, because the colorectal level of AA tended to be lower in DSS-treated *Pla2g10*$^{-/-}$ mice than in WT mice (Fig. 8*A*), the ω3 PUFA metabolites were present at 30 times lower than the AA metabolites (Fig. 8, *B* and *C*), and AA suppressed IL-17A release by LPLs (Fig. 8*D*), it is possible that AA itself released by sPLA$_2$-X might also contribute to the protection from colitis and that the background level of PGs might mask a pool of PGs potentially formed following mobilization of AA by sPLA$_2$-X in a subset of cells.

Protective Role of the cPLA$_2$α-PGE$_2$ Axis against Colitis—The above observations prompted us to ask which PLA$_2$ subtype(s) is linked to AA metabolism in colitis. We therefore applied the DSS-induced colitis model to mice null for *Pla2g4a* and *Pla2g6*, which are expressed in the colon (Fig. 4*A*). Severe weight gain, fecal bleeding, and diarrhea were seen in *Pla2g4a*$^{-/-}$ mice, but not WT mice, soon after oral application of DSS (Fig. 9, *A* and *B*). On day 7, colorectal damage with epithelial loss and massive immune cell infiltration (Fig. 9*C*), splenomegaly (Fig. 9*D*), and decrease of hematocrit (Fig. 9*E*) were far more prominent in *Pla2g4a*$^{-/-}$ mice than in WT mice. In contrast, exacerbation of these parameters was not evident in *Pla2g6*$^{-/-}$ mice (Fig. 9, *A* and *B*). The overall phenotypes in *Pla2g4a*$^{-/-}$ mice were similar to those in *Ptger4*$^{-/-}$ mice, which lack the PGE$_2$ receptor

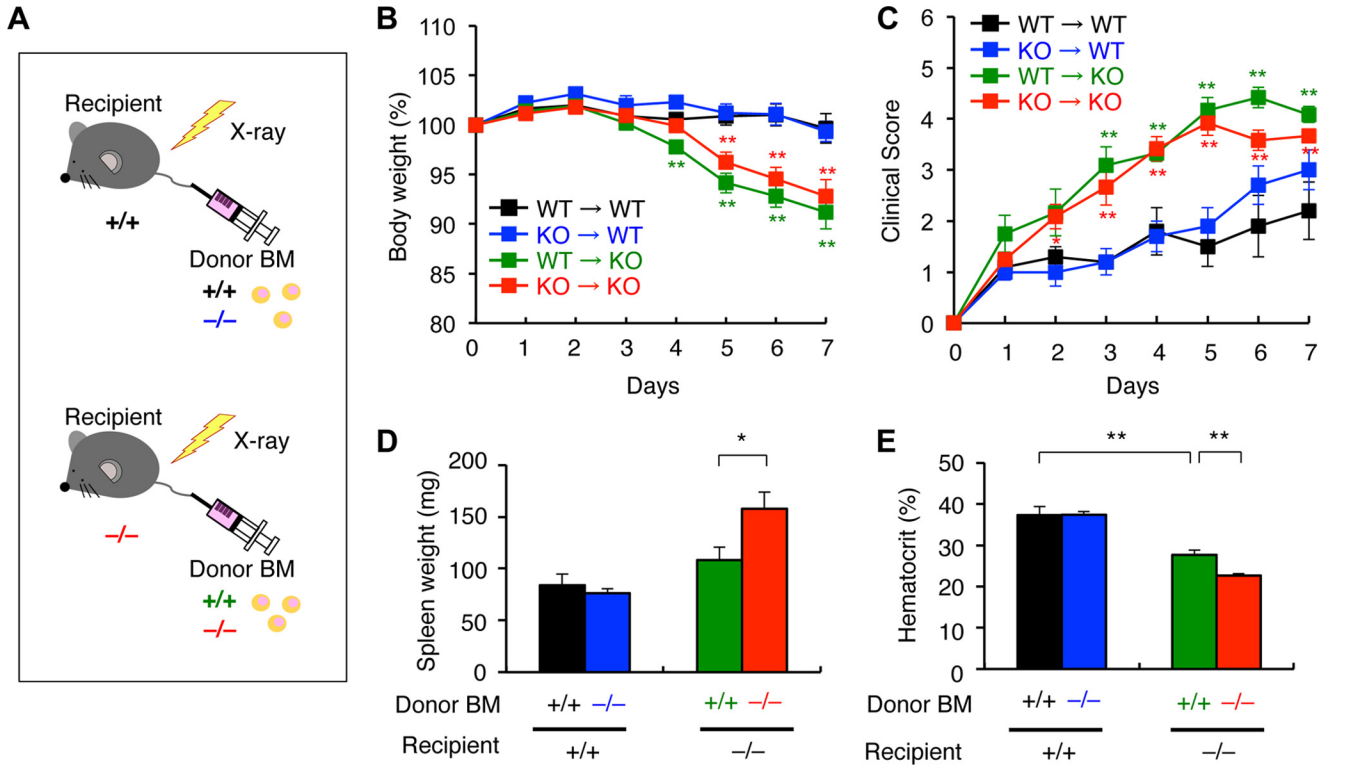

FIGURE 7. **Evaluation of the role of hematopoietic or non-hematopoietic sPLA$_2$-X in DSS-induced colitis by BM transfer.** *A*, experimental procedure used for BM transfer. *B* and *C*, daily monitoring of body weight (*B*) and clinical score (*C*) in the indicated groups that were administered with 1% DSS orally ($n = 5–6$, **, $p < 0.01$ *versus* WT → WT). *D* and *E*, spleen weight (*D*) and hematocrit (*E*) in the indicated groups after oral administration of DSS for 7 days ($n = 5–6$, *, $p < 0.05$, and **, $p < 0.01$). Values are mean ± S.E.

EP4 (31), or *Ptges*$^{-/-}$ mice, which lack microsomal PGE$_2$ synthase-1 (mPGES-1) (Fig. 9, *A–E*) (52), even though the overall symptoms, as revealed by the delay in body weight loss, were milder in *Ptges*$^{-/-}$ mice than in *Pla2g4a*$^{-/-}$ mice.

Lipidomics studies of the colon revealed that PGE$_2$ was present at a markedly lower level in DSS-treated *Pla2g4a*$^{-/-}$ mice than in WT mice (Fig. 9*F*). 12-HHT was also ~50% lower, although the changes in other prostanoids were relatively small, in DSS-treated *Pla2g4a*$^{-/-}$ mice compared with WT mice. These results indicate that cPLA$_2\alpha$ is preferentially coupled with PGE$_2$ and to a lesser extent 12-HHT in DSS-induced colitis. In contrast, the levels of EPA and DHA metabolites were unaffected by *Pla2g4a* deficiency. The level of PGE$_2$ was markedly decreased in *Ptges*$^{-/-}$ mice (to a level similar to that in *Pla2g4a*$^{-/-}$ mice, but not to zero), with reciprocal increases of other prostanoids, relative to WT mice (Fig. 9*F*). These results suggest the following. (i) The severe exacerbation of DSS-induced colitis in *Pla2g4a*$^{-/-}$ mice is due to the marked reduction of colon-protective prostanoids such as PGE$_2$ and 12-HHT (31, 45, 46). (ii) The milder outcome in *Ptges*$^{-/-}$ mice than in *Pla2g4a*$^{-/-}$ mice is probably because the former harbors the reduction of PGE$_2$ only, which may be counterbalanced by the increases in 12-HHT and/or other prostanoids through a shunting effect (53). (iii) The cPLA$_2\alpha$-mPGES-1 axis accounts mostly, if not entirely, for a pool of PGE$_2$ responsible for this disease model. (iv) There is an alternative route for the basal, cPLA$_2\alpha$-independent production of prostanoids such as PGF$_{2\alpha}$ and 6-keto-PGF$_{1\alpha}$ (a stable end product of PGI$_2$) in the colon. Overall, cPLA$_2\alpha$ and sPLA$_2$-X exert a protective effect against colitis by mobilizing distinct sets of lipid metabolites, *i.e.* ω6 AA and ω3 PUFA metabolites, respectively.

Reduced Release of DHA and DPA in Pla2g10$^{-/-}$ *Spermatozoa*—In addition to the GI tract, sPLA$_2$-X is abundantly expressed in the testis, being stored in and released from the acrosomes of spermatozoa during capacitation and the acrosome reaction, and *Pla2g10*$^{-/-}$ spermatozoa display reduced fertility, with no alteration in motility (40, 54). However, the phospholipid metabolism underlying the action of sPLA$_2$-X in this context remains to be determined.

To address this issue, we performed lipidomics analysis of *Pla2g10*$^{+/+}$ and *Pla2g10*$^{-/-}$ spermatozoa before and after capacitation. Consistent with the view that sPLA$_2$-X is dispensable for sperm maturation (40), the PC compositions of spermatozoa before capacitation were identical between the genotypes (Fig. 10*A*). Notably, after capacitation, the levels of PC species with DHA or DPA, but not those with AA and other fatty acids, were significantly lower in *Pla2g10*$^{+/+}$ cells than in *Pla2g10*$^{-/-}$ cells (Fig. 10*A*). In accordance with this, the release of DHA and DPA but not AA and linoleic acid (Fig. 10*B*), as well as LPC with C18:0 (and to a lesser extent with C18:1 and C16:0) (Fig. 10*C*), was greater in *Pla2g10*$^{+/+}$ than in *Pla2g10*$^{-/-}$ spermatozoa. Release of EPA was very low, because EPA-bearing PC was a minor phospholipid component in mouse sperm (Fig. 10, *A* and *B*) (3). These results suggest that sPLA$_2$-X secreted from activated spermatozoa preferentially cleaves DHA- or DPA-containing PC in the sperm membrane to release DHA, DPA, and LPC.

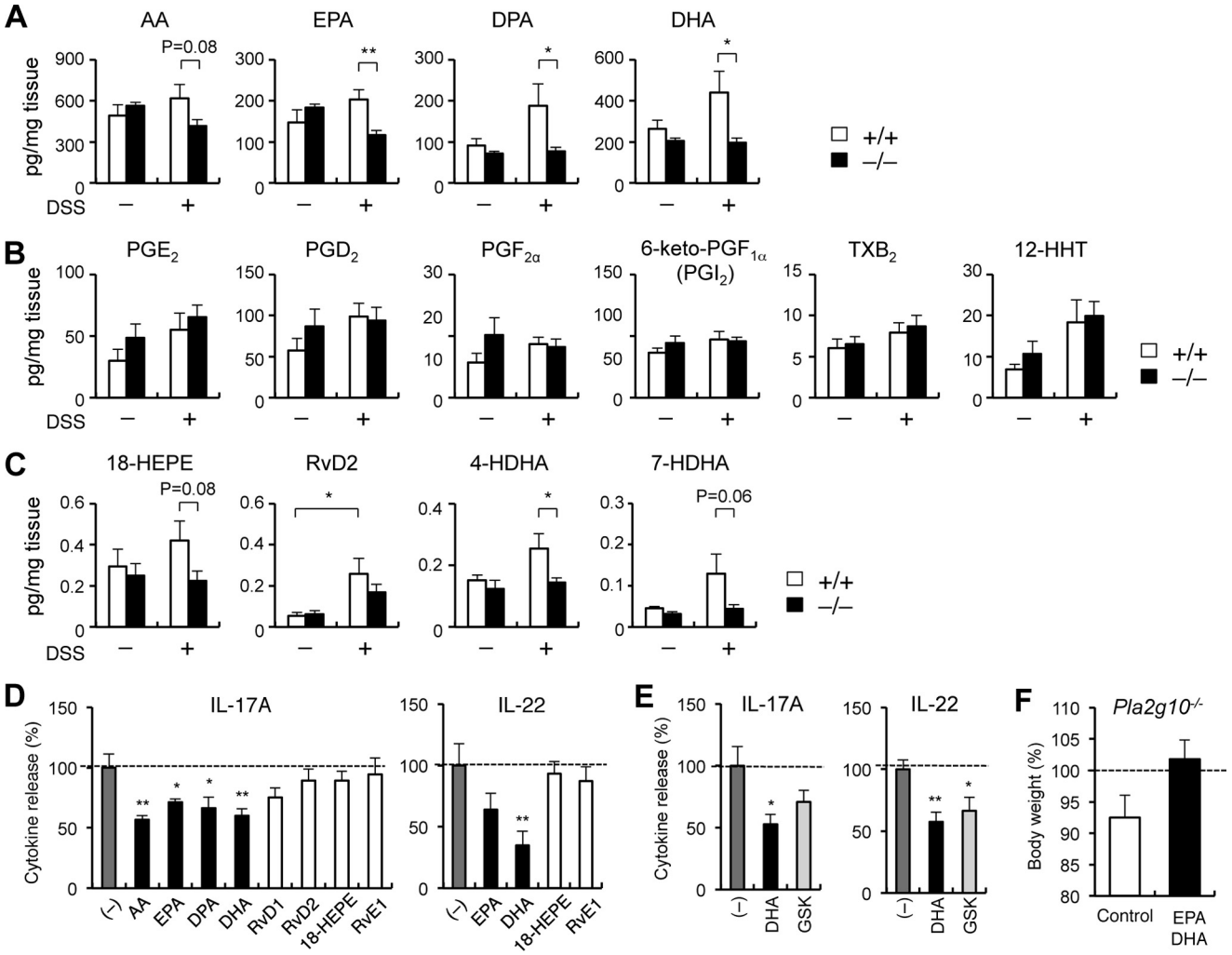

FIGURE 8. **ESI-MS profiling of PUFA metabolites in DSS-induced colitis.** *A–C*, ESI-MS analysis of PUFAs (*A*), AA metabolites (*B*), and EPA/DHA metabolites (*C*) in the colon of *Pla2g10*$^{+/+}$ and *Pla2g10*$^{-/-}$ mice with or without administration of 1% DSS for 7 days ($n = 6–7$; *, $p < 0.05$, and **, $p < 0.01$). *D* and *E*, effects of PUFAs and their metabolites (*D*) or GSK137647 (*GSK*; a GPR120 agonist) (*E*) on Th17 cytokine production by LPLs isolated from DSS-treated WT mice ($n = 4$; *, $p < 0.05$, and **, $p < 0.01$ *versus* without treatment with lipids or GSK137647). Results are expressed as percentages, with values in the absence of lipids or GSK137647 as 100% (*dashed line*). *F*, effects of intrarectal injection of ω3 PUFAs on body weight loss of *Pla2g10*$^{-/-}$ mice treated with 1% DSS for 5 days ($n = 3$). Results are expressed as percentages, with the value of DSS-untreated mice as 100% (*dashed line*). Values are mean ± S.E. *HEPE*, hydroxyeicosapentaenoic acid; *HDHA*, hydroxydocosahexaenoic acid; *TXB$_2$*, thromboxane B$_2$.

We then evaluated the effects of these lipid products on fertilization. The fertilization ability of *Pla2g10*$^{-/-}$ sperm with WT oocytes was lower than that of *Pla2g10*$^{+/+}$ sperm, as reported previously (40, 54), whereas addition of DPA and to a lesser extent LPC restored the fertilization ability of *Pla2g10*$^{-/-}$ sperm (Fig. 10*D*). Thus, the lipid products released from the sperm membrane by sPLA$_2$-X, particularly DPA, facilitate optimal fertilization.

Discussion

The roles of sPLA$_2$s, including sPLA$_2$-X, in promoting or attenuating inflammation or other pathophysiological events may be dictated by the cells from which they are secreted, the target membranes on which they act, or when and how their phospholipid-hydrolytic products are associated with the particular biological processes in cell-, tissue-, or disease-specific contexts. Given the current proposal that sPLA$_2$-X is a pro-inflammatory enzyme (2, 16–22), our present observation that *PLA2G10*$^{tg/+}$ mice exhibited a global immunosuppressive phenotype was initially unexpected but appeared to be compatible with studies reporting that sPLA$_2$-X overexpression in cultured macrophages elicited anti-inflammatory responses (23) and that atherosclerosis worsened in *Ldlr*$^{-/-}$ mice that had been received *Pla2g10*$^{-/-}$ BM cells by adoptive transfer (24). In this study, by employing *Pla2g10* gene-manipulated mice in combination with lipidomics, we have revealed the anti-inflammatory, rather than pro-inflammatory, features of sPLA$_2$-X *in vivo*.

Endogenous sPLA$_2$-X is constitutively expressed at a high level in the GI tract and testis (40, 41, 54), and this study using *Pla2g10*$^{-/-}$ mice has shown that sPLA$_2$-X mobilizes ω3 PUFAs in addition to, or even in favor of, ω6 AA in these tissues in the processes of colitis and fertilization, respectively. Even in *PLA2G10*$^{tg/+}$ mice, which globally overexpress human sPLA$_2$-X at a super-physiological level, there are modest trends toward selective increases of ω3 PUFA metabolites over ω6 AA metabolites in multiple if not all tissues. These observations suggest that sPLA$_2$-X has the intrinsic ability to mobilize ω3 PUFA-derived metabolites *in vivo*. We have

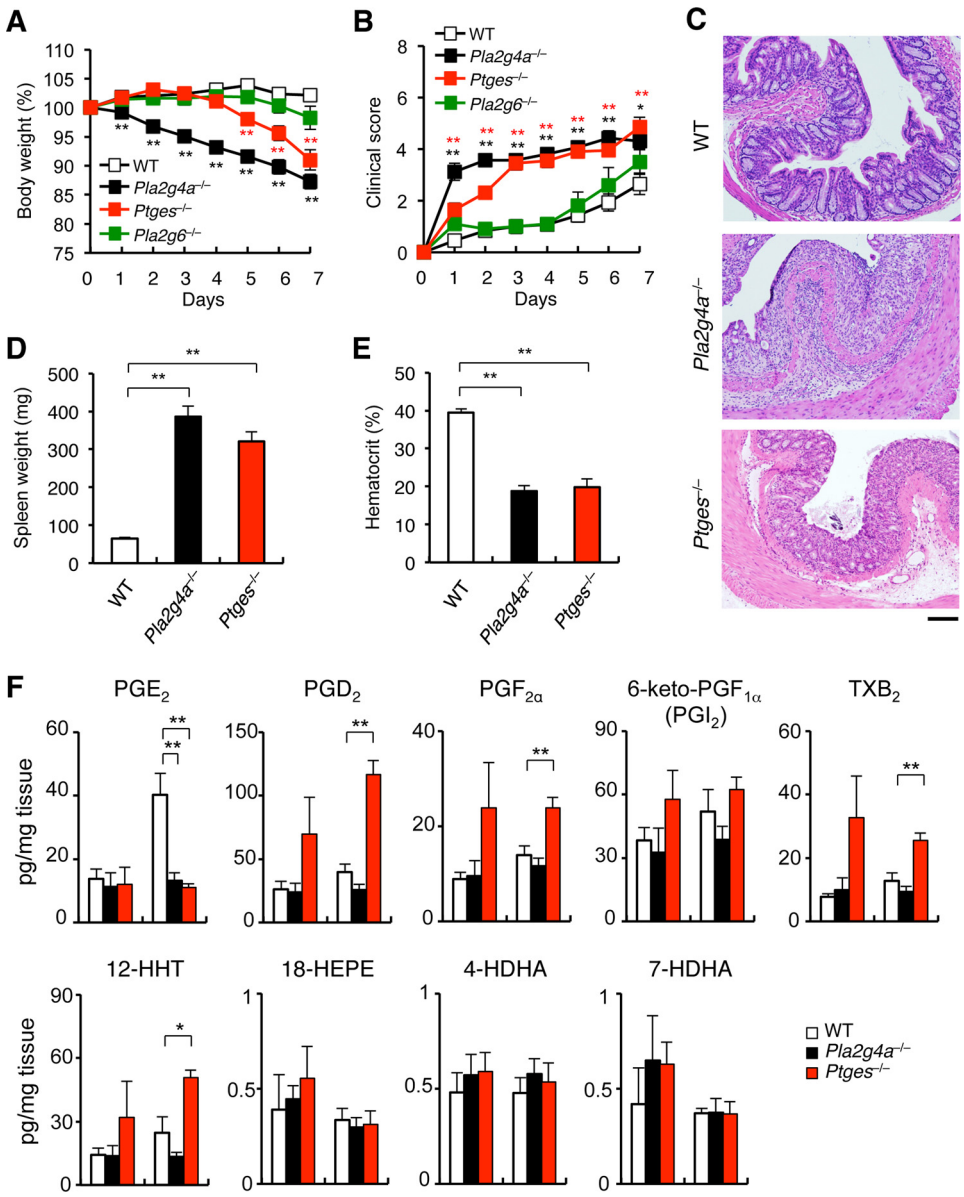

FIGURE 9. **DSS-induced colitis in *Pla2g4a*$^{-/-}$, *Pla2g6*$^{-/-}$, and *Ptges*$^{-/-}$ mice.** WT ($n = 9$), *Pla2g4a*$^{-/-}$ ($n = 4$), *Pla2g6*$^{-/-}$ ($n = 5$), and *Ptges*$^{-/-}$ ($n = 10$) mice were administered 1% DSS orally. Body weight (*A*) and clinical score (*B*) were monitored at the indicated times, and colon histology (*bar,* 100 μm) (*C*), spleen weight (*D*), hematocrit (*E*), and ES-MS profiles of colorectal lipids (*F*) were evaluated at day 7. There were no differences in the measured parameters among the genotypes under normal conditions (data not shown). Mean ± S.E., *, $p < 0.05$, and **, $p < 0.01$.

recently shown that sPLA$_2$-IID, which is highly expressed in dendritic cells in lymphoid tissues, resolves contact hypersensitivity by mobilizing DHA-derived pro-resolving lipid mediators (5). Our results thus reveal a novel role of sPLA$_2$-X as another ω3 PUFA-mobilizing sPLA$_2$, thereby regulating tissue-specific homeostasis.

ω3 PUFAs such as EPA and DHA resolve various types of inflammation, obesity, and atherosclerosis by acting on fatty acid-sensing receptors (*e.g.* PPARs and GPR120; see below) (51, 55), by being metabolized to pro-resolving lipid mediators (*e.g.* resolvins and protectins) (38, 39), by attenuating endoplasmic reticulum stress (56), or by increasing membrane fluidity, thus eventually altering membrane signaling or trafficking (57). It is likely that the anti-inflammatory actions of sPLA$_2$-X occur through any of these mechanisms. Indeed, changes in the tissue levels of ω3 PUFAs and their metabolites are correlated with the levels of sPLA$_2$-X expression. ω3 PUFA metabolites promote M2 macrophage polarization (58, 59), prevent T cell activation or differentiation (60, 61), and alter antibody production by B cells (62), a view that is relevant to the phenotypes observed in *PLA2G10*$^{tg/+}$ mice. Our results are also in accord with the aggravating role of sPLA$_2$-X in asthma (2), where M2 macrophages are associated with the Th2-skewed airway inflammation (13). Therefore, we speculate that the reported roles of sPLA$_2$-X in protection against atherosclerosis and obesity (24, 63) may also involve, at least in part, the mobilization of ω3 PUFAs by this enzyme in a local tissue or even at a distal site (*e.g.* the GI tract), thus affecting the disease indirectly.

Our results do not rule out the contribution of sPLA$_2$-X to AA metabolism, because this enzyme can release AA in various cultured cells (at 10–100 ng/ml or more) (16–18), and because several *in vivo* studies have shown that *Pla2g10* ablation results

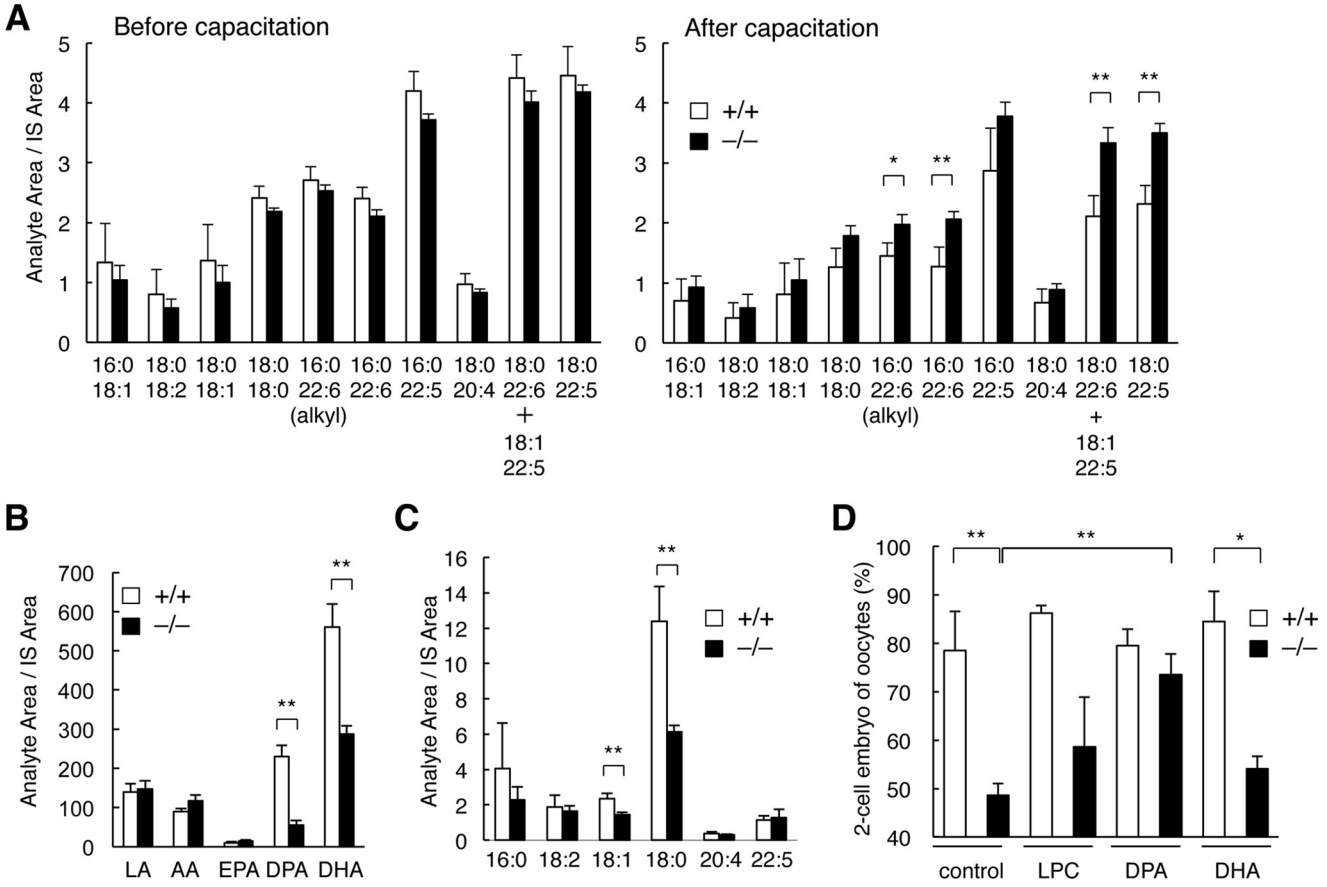

FIGURE 10. **sPLA$_2$-X mobilizes DPA, DHA, and LPC from the sperm membrane.** *A,* ESI-MS of PC molecular species in spermatozoa from 8-week-old *Pla2g10*$^{+/+}$ and *Pla2g10*$^{-/-}$ mice before and after capacitation ($n = 4–6$). *B* and *C,* ESI-MS of PUFAs (*B*) and LPC species (*C*) released from *Pla2g10*$^{+/+}$ and *Pla2g10*$^{-/-}$ spermatozoa after capacitation ($n = 4$). *LA,* linoleic acid. *D,* effects of the indicated lipids (1 μM) on *in vitro* fertilization ability of *Pla2g10*$^{+/+}$ and *Pla2g10*$^{-/-}$ spermatozoa with WT oocytes ($n = 3$). Mean ± S.E., *, $p < 0.05$, and **, $p < 0.01$.

in reduction of eicosanoids (2, 19–22). However, many of the previous *in vivo* studies did not measure ω3 PUFA metabolites or discriminate whether sPLA$_2$-X directly mobilizes eicosanoids or whether the observed changes in eicosanoids reflected changes in cPLA$_2$α expression or activation in the ongoing process of a given pathology. In fact, in the context of asthma, sPLA$_2$-X secreted from the airway epithelium acts on infiltrating eosinophils in a paracrine manner to produce LPC, which in turn increases Ca^{2+} influx leading to cPLA$_2$α-dependent leukotriene generation (64), although it may directly mobilize AA metabolites from lung epithelial cells in an autocrine manner (20). In this study, we have shown that cPLA$_2$α and sPLA$_2$-X are functionally segregated in the large intestine, driving non-overlapping lipid pathways (ω6 AA metabolism and ω3 PUFA metabolism, respectively), which eventually culminates in a common outcome, *i.e.* protection against colitis. To the best of our knowledge, this is the first demonstration of the PLA$_2$ enzymes that are responsible for the release of distinct PUFAs in IBD. Moreover, the sPLA$_2$-X-driven ω3 PUFAs are capable of suppressing Th17 cytokine production by intestinal LPLs through GPR120, providing the first evidence for the functional linkage from a particular sPLA$_2$ to a fatty acid receptor. Although our study failed to show the ameliorating effect of resolvins and 18-HEPE on Th17 cytokine production by these cells, it is possible that these pro-resolving mediators could affect other steps of colitis, for instance by acting directly on epithelial cells to protect from injuries and on neutrophils to suppress their migration and to promote their clearance. In fact, resolvins block colitis when administered exogenously (47–49), and an endogenous EPA-derived epoxide attenuates allergic colitis (65).

Presumably, the mobilization of ω6 AA *versus* ω3 PUFA metabolites, or even other fatty acids and lysophospholipids, by sPLA$_2$-X or other sPLA$_2$s would rely not only on their intrinsic enzymatic properties but also on tissue- or disease-specific contexts such as the lipid composition of target membranes or the spatiotemporal availability of downstream enzymes, which may explain why the same enzyme often exerts pro- or anti-inflammatory effects with different lipid mediator profiles in distinct settings. Indeed, sPLA$_2$-IID mobilizes DHA-derived RvD1 in draining lymph nodes to suppress contact dermatitis (5) and AA-derived PGD$_2$ in the lung to counteract anti-viral immunity (66). sPLA$_2$-V in adipose tissue releases oleic acid from lipoproteins in the process of obesity (8). Moreover, mobilization of a particular class of lysophospholipids, rather than fatty acids, is important for the function of sPLA$_2$-IIF in the epidermis (67). Thus, caution should be exercised when interpreting the results of studies in which the actions of sPLA$_2$ are assigned only to AA metabolism.

Apart from their roles in inflammation, multiple sPLA$_2$s are expressed in male genital organs (68), among which two particular isoforms, sPLA$_2$-III and -X, participate in sperm maturation and activation, respectively (3, 54). Several lines of evidence suggest that DHA insufficiency causes asthenozoospermia with hypomotility and infertility (69, 70). sPLA$_2$-III is secreted from the epididymal epithelium and acts on immature spermatozoa passing through the epididymal duct to promote sperm membrane remodeling (3). As such, mature spermatozoa gain a higher proportion of DPA/DHA-containing PC species, which are crucial for sperm motility and thereby fertility. After ejaculation into the female duct, mature sperm undergo capacitation to allow hypermotility and acrosome reaction for fertilization, where the acrosome-derived sPLA$_2$-X plays a promoting role (54). DPA, an intermediate in the biosynthetic conversion from EPA to DHA, has recently attracted attention as a precursor of novel 13-series resolvins with potent pro-resolving activity (71). Beyond this function, DPA is highly enriched in sperm cells, yet the biological importance of this PUFA in reproduction has been poorly understood (72). We now provide evidence that sPLA$_2$-X selectively hydrolyzes DPA/DHA-containing PC species in sperm membranes to release DPA, DHA, and LPC, among which DPA has the highest ability to restore the fertilization ability of *Pla2g10*$^{-/-}$ sperm. Although the mechanism underlying this action of DPA still awaits future studies, our results nonetheless provide new insight into the biological role of this unique PUFA in reproduction and also a rationale for its high degree of enrichment in sperm cells. Thus, sPLA$_2$-III promotes epididymal sperm maturation, allowing enrichment of DPA/DHA-containing PC species in sperm membranes, and then sPLA$_2$-X acts on these phospholipids to release DPA for successful fertilization, thereby underscoring an elegant cooperation of the two sPLA$_2$s in the process of male reproduction.

Author Contributions—M. M. conceived and coordinated the study and wrote the paper. R. M. and Y. T. designed, performed, and analyzed the experiments shown in Figs. 4–9. K. Y., H. S., A. U., and K. I. designed, performed, and analyzed the experiments shown in Figs. 1–3 and 10. Y. N. designed, performed, and analyzed microarray experiments. T. K. and T. Y. provided technical advice. All authors reviewed the results and approved the final version of the manuscript.

Acknowledgments—We thank Dr. M. H. Gelb (University of Washington) for providing Pla2g2d$^{-/-}$*, Pla2g2e*$^{-/-}$*, and Pla2g2f*$^{-/-}$ *mice; Dr. T. Shimizu and Y. Kita (National Center for Global Health and Medicine and the University of Tokyo) for providing Pla2g4a*$^{-/-}$ *mice; Dr. J. P. Arm for providing Pla2g5*$^{-/-}$ *mice (Novartis Pharma); Dr. K. Shinzawa (Osaka University) for providing Pla2g6*$^{-/-}$ *mice; Drs. K. Hanasaki and Y. Yokota (Shionogi Pharmaceutical, Osaka, Japan) for providing Pla2g10*$^{-/-}$ *mice; and for Dr. S. Akira (Osaka University) for providing Ptges*$^{-/-}$ *mice.*

References

1. Lambeau, G., and Gelb, M. H. (2008) Biochemistry and physiology of mammalian secreted phospholipases A$_2$. *Annu. Rev. Biochem.* **77,** 495–520
2. Henderson, W. R., Jr., Chi, E. Y., Bollinger, J. G., Tien, Y. T., Ye, X., Castelli, L., Rubtsov, Y. P., Singer, A. G., Chiang, G. K., Nevalainen, T., Rudensky, A. Y., and Gelb, M. H. (2007) Importance of group X-secreted phospholipase A$_2$ in allergen-induced airway inflammation and remodeling in a mouse asthma model. *J. Exp. Med.* **204,** 865–877
3. Sato, H., Taketomi, Y., Isogai, Y., Miki, Y., Yamamoto, K., Masuda, S., Hosono, T., Arata, S., Ishikawa, Y., Ishii, T., Kobayashi, T., Nakanishi, H., Ikeda, K., Taguchi, R., Hara, S., *et al.* (2010) Group III secreted phospholipase A$_2$ regulates epididymal sperm maturation and fertility in mice. *J. Clin. Invest.* **120,** 1400–1414
4. Yamamoto, K., Taketomi, Y., Isogai, Y., Miki, Y., Sato, H., Masuda, S., Nishito, Y., Morioka, K., Ishimoto, Y., Suzuki, N., Yokota, Y., Hanasaki, K., Ishikawa, Y., Ishii, T., Kobayashi, T., *et al.* (2011) Hair follicular expression and function of group X secreted phospholipase A$_2$ in mouse skin. *J. Biol. Chem.* **286,** 11616–11631
5. Miki, Y., Yamamoto, K., Taketomi, Y., Sato, H., Shimo, K., Kobayashi, T., Ishikawa, Y., Ishii, T., Nakanishi, H., Ikeda, K., Taguchi, R., Kabashima, K., Arita, M., Arai, H., Lambeau, G., *et al.* (2013) Lymphoid tissue phospholipase A$_2$ group IID resolves contact hypersensitivity by driving antiinflammatory lipid mediators. *J. Exp. Med.* **210,** 1217–1234
6. Taketomi, Y., Ueno, N., Kojima, T., Sato, H., Murase, R., Yamamoto, K., Tanaka, S., Sakanaka, M., Nakamura, M., Nishito, Y., Kawana, M., Kambe, N., Ikeda, K., Taguchi, R., Nakamizo, S., *et al.* (2013) Mast cell maturation is driven via a group III phospholipase A$_2$-prostaglandin D$_2$-DP1 receptor paracrine axis. *Nat. Immunol.* **14,** 554–563
7. Boudreau, L. H., Duchez, A. C., Cloutier, N., Soulet, D., Martin, N., Bollinger, J., Paré, A., Rousseau, M., Naika, G. S., Lévesque, T., Laflamme, C., Marcoux, G., Lambeau, G., Farndale, R. W., Pouliot, M., *et al.* (2014) Platelets release mitochondria serving as substrate for bactericidal group IIA-secreted phospholipase A$_2$ to promote inflammation. *Blood* **124,** 2173–2183
8. Sato, H., Taketomi, Y., Ushida, A., Isogai, Y., Kojima, T., Hirabayashi, T., Miki, Y., Yamamoto, K., Nishito, Y., Kobayashi, T., Ikeda, K., Taguchi, R., Hara, S., Ida, S., Miyamoto, Y., *et al.* (2014) The adipocyte-inducible secreted phospholipases PLA2G5 and PLA2G2E play distinct roles in obesity. *Cell Metab.* **20,** 119–132
9. Murakami, M., Taketomi, Y., Miki, Y., Sato, H., Hirabayashi, T., and Yamamoto, K. (2011) Recent progress in phospholipase A$_2$ research: from cells to animals to humans. *Prog. Lipid Res.* **50,** 152–192
10. Murakami, M., Sato, H., Miki, Y., Yamamoto, K., and Taketomi, Y. (2015) A new era of secreted phospholipase A$_2$. *J. Lipid Res.* **56,** 1248–1261
11. Pernet, E., Guillemot, L., Burgel, P. R., Martin, C., Lambeau, G., Sermet-Gaudelus, I., Sands, D., Leduc, D., Morand, P. C., Jeammet, L., Chignard, M., Wu, Y., and Touqui, L. (2014) Pseudomonas aeruginosa eradicates *Staphylococcus aureus* by manipulating the host immunity. *Nat. Commun.* **5,** 5105
12. Rubio, J. M., Rodríguez, J. P., Gil-de-Gómez, L., Guijas, C., Balboa, M. A., and Balsinde, J. (2015) Group V secreted phospholipase A$_2$ is upregulated by IL-4 in human macrophages and mediates phagocytosis via hydrolysis of ethanolamine phospholipids. *J. Immunol.* **194,** 3327–3339
13. Ohta, S., Imamura, M., Xing, W., Boyce, J. A., and Balestrieri, B. (2013) Group V secretory phospholipase A$_2$ is involved in macrophage activation and is sufficient for macrophage effector functions in allergic pulmonary inflammation. *J. Immunol.* **190,** 5927–5938
14. Boilard, E., Lai, Y., Larabee, K., Balestrieri, B., Ghomashchi, F., Fujioka, D., Gobezie, R., Coblyn, J. S., Weinblatt, M. E., Massarotti, E. M., Thornhill, T. S., Divangahi, M., Remold, H., Lambeau, G., Gelb, M. H., *et al.* (2010) A novel anti-inflammatory role for secretory phospholipase A$_2$ in immune complex-mediated arthritis. *EMBO Mol. Med.* **2,** 172–187
15. Balestrieri, B., Maekawa, A., Xing, W., Gelb, M. H., Katz, H. R., and Arm, J. P. (2009) Group V secretory phospholipase A$_2$ modulates phagosome maturation and regulates the innate immune response against *Candida albicans*. *J. Immunol.* **182,** 4891–4898
16. Murakami, M., Koduri, R. S., Enomoto, A., Shimbara, S., Seki, M., Yoshihara, K., Singer, A., Valentin, E., Ghomashchi, F., Lambeau, G., Gelb, M. H., and Kudo, I. (2001) Distinct arachidonate-releasing functions of mammalian secreted phospholipase A$_2$s in human embryonic kidney 293 and rat mastocytoma RBL-2H3 cells through heparan sulfate shuttling and external plasma membrane mechanisms. *J. Biol. Chem.* **276,**

10083–10096
17. Bezzine, S., Koduri, R. S., Valentin, E., Murakami, M., Kudo, I., Ghomashchi, F., Sadilek, M., Lambeau, G., and Gelb, M. H. (2000) Exogenously added human group X secreted phospholipase A_2 but not the group IB, IIA, and V enzymes efficiently release arachidonic acid from adherent mammalian cells. *J. Biol. Chem.* **275,** 3179–3191
18. Hanasaki, K., Ono, T., Saiga, A., Morioka, Y., Ikeda, M., Kawamoto, K., Higashino, K., Nakano, K., Yamada, K., Ishizaki, J., and Arita, H. (1999) Purified group X secretory phospholipase A_2 induced prominent release of arachidonic acid from human myeloid leukemia cells. *J. Biol. Chem.* **274,** 34203–34211
19. Kelvin, A. A., Degousee, N., Banner, D., Stefanski, E., León, A. J., Angoulvant, D., Paquette, S. G., Huang, S. S., Danesh, A., Robbins, C. S., Noyan, H., Husain, M., Lambeau, G., Gelb, M., Kelvin, D. J., *et al.* (2014) Lack of group X secreted phospholipase A_2 increases survival following pandemic H1N1 influenza infection. *Virology* **454,** 78–92
20. Hallstrand, T. S., Lai, Y., Altemeier, W. A., Appel, C. L., Johnson, B., Frevert, C. W., Hudkins, K. L., Bollinger, J. G., Woodruff, P. G., Hyde, D. M., Henderson, W. R., Jr., and Gelb, M. H. (2013) Regulation and function of epithelial secreted phospholipase A_2 group X in asthma. *Am. J. Respir. Crit. Care Med.* **188,** 42–50
21. Watanabe, K., Fujioka, D., Saito, Y., Nakamura, T., Obata, J. E., Kawabata, K., Watanabe, Y., Mishina, H., Tamaru, S., Hanasaki, K., and Kugiyama, K. (2012) Group X secretory PLA_2 in neutrophils plays a pathogenic role in abdominal aortic aneurysms in mice. *Am. J. Physiol. Heart Circ. Physiol.* **302,** H95–H104
22. Fujioka, D., Saito, Y., Kobayashi, T., Yano, T., Tezuka, H., Ishimoto, Y., Suzuki, N., Yokota, Y., Nakamura, T., Obata, J. E., Kanazawa, M., Kawabata, K., Hanasaki, K., and Kugiyama, K. (2008) Reduction in myocardial ischemia/reperfusion injury in group X secretory phospholipase A_2-deficient mice. *Circulation* **117,** 2977–2985
23. Curfs, D. M., Ghesquiere, S. A., Vergouwe, M. N., van der Made, I., Gijbels, M. J., Greaves, D. R., Verbeek, J. S., Hofker, M. H., and de Winther, M. P. (2008) Macrophage secretory phospholipase A_2 group X enhances anti-inflammatory responses, promotes lipid accumulation, and contributes to aberrant lung pathology. *J. Biol. Chem.* **283,** 21640–21648
24. Ait-Oufella, H., Herbin, O., Lahoute, C., Coatrieux, C., Loyer, X., Joffre, J., Laurans, L., Ramkhelawon, B., Blanc-Brude, O., Karabina, S., Girard, C. A., Payré, C., Yamamoto, K., Binder, C. J., Murakami, M., *et al.* (2013) Group X secreted phospholipase A_2 limits the development of atherosclerosis in LDL receptor-null mice. *Arterioscler. Thromb. Vasc. Biol.* **33,** 466–473
25. Sato, H., Kato, R., Isogai, Y., Saka, G., Ohtsuki, M., Taketomi, Y., Yamamoto, K., Tsutsumi, K., Yamada, J., Masuda, S., Ishikawa, Y., Ishii, T., Kobayashi, T., Ikeda, K., Taguchi, R., *et al.* (2008) Analyses of group III secreted phospholipase A_2 transgenic mice reveal potential participation of this enzyme in plasma lipoprotein modification, macrophage foam cell formation, and atherosclerosis. *J. Biol. Chem.* **283,** 33483–33497
26. Mitsuishi, M., Masuda, S., Kudo, I., and Murakami, M. (2007) Human group III phospholipase A_2 suppresses adenovirus infection into host cells. Evidence that group III, V and X phospholipase A_2s act on distinct cellular phospholipid molecular species. *Biochim. Biophys. Acta* **1771,** 1389–1396
27. Uozumi, N., Kume, K., Nagase, T., Nakatani, N., Ishii, S., Tashiro, F., Komagata, Y., Maki, K., Ikuta, K., Ouchi, Y., Miyazaki, J., and Shimizu, T. (1997) Role of cytosolic phospholipase A_2 in allergic response and parturition. *Nature* **390,** 618–622
28. Satake, Y., Diaz, B. L., Balestrieri, B., Lam, B. K., Kanaoka, Y., Grusby, M. J., and Arm, J. P. (2004) Role of group V phospholipase A_2 in zymosan-induced eicosanoid generation and vascular permeability revealed by targeted gene disruption. *J. Biol. Chem.* **279,** 16488–16494
29. Shinzawa, K., Sumi, H., Ikawa, M., Matsuoka, Y., Okabe, M., Sakoda, S., and Tsujimoto, Y. (2008) Neuroaxonal dystrophy caused by group VIA phospholipase A_2 deficiency in mice: a model of human neurodegenerative disease. *J. Neurosci.* **28,** 2212–2220
30. Kamei, D., Yamakawa, K., Takegoshi, Y., Mikami-Nakanishi, M., Nakatani, Y., Oh-Ishi, S., Yasui, H., Azuma, Y., Hirasawa, N., Ohuchi, K., Kawaguchi, H., Ishikawa, Y., Ishii, T., Uematsu, S., Akira, S., *et al.* (2004) Reduced pain hypersensitivity and inflammation in mice lacking microsomal prostaglandin E synthase-1. *J. Biol. Chem.* **279,** 33684–33695
31. Kabashima, K., Saji, T., Murata, T., Nagamachi, M., Matsuoka, T., Segi, E., Tsuboi, K., Sugimoto, Y., Kobayashi, T., Miyachi, Y., Ichikawa, A., and Narumiya, S. (2002) The prostaglandin receptor EP4 suppresses colitis, mucosal damage and CD4 cell activation in the gut. *J. Clin. Invest.* **109,** 883–893
32. Odegaard, J. I., and Chawla, A. (2013) The immune system as a sensor of the metabolic state. *Immunity* **38,** 644–654
33. Taylor, N. (2010) CCR7/CCR9: knockin' on the thymus door. *Blood* **115,** 1861–1862
34. Cyster, J. G. (2009) Settling the thymus: immigration requirements. *J. Exp. Med.* **206,** 731–734
35. Sun, Z., Unutmaz, D., Zou, Y. R., Sunshine, M. J., Pierani, A., Brenner-Morton, S., Mebius, R. E., and Littman, D. R. (2000) Requirement for RORγ in thymocyte survival and lymphoid organ development. *Science* **288,** 2369–2373
36. Carlson, C. M., Endrizzi, B. T., Wu, J., Ding, X., Weinreich, M. A., Walsh, E. R., Wani, M. A., Lingrel, J. B., Hogquist, K. A., and Jameson, S. C. (2006) Kruppel-like factor 2 regulates thymocyte and T-cell migration. *Nature* **442,** 299–302
37. Zaldumbide, A., Carlotti, F., Pognonec, P., and Boulukos, K. E. (2002) The role of the Ets2 transcription factor in the proliferation, maturation, and survival of mouse thymocytes. *J. Immunol.* **169,** 4873–4881
38. Serhan, C. N. (2014) Pro-resolving lipid mediators are leads for resolution physiology. *Nature* **510,** 92–101
39. Buckley, C. D., Gilroy, D. W., and Serhan, C. N. (2014) Proresolving lipid mediators and mechanisms in the resolution of acute inflammation. *Immunity* **40,** 315–327
40. Sato, H., Isogai, Y., Masuda, S., Taketomi, Y., Miki, Y., Kamei, D., Hara, S., Kobayashi, T., Ishikawa, Y., Ishii, T., Ikeda, K., Taguchi, R., Ishimoto, Y., Suzuki, N., Yokota, Y., *et al.* (2011) Physiological roles of group X-secreted phospholipase A_2 in reproduction, gastrointestinal phospholipid digestion, and neuronal function. *J. Biol. Chem.* **286,** 11632–11648
41. Surrel, F., Jemel, I., Boilard, E., Bollinger, J. G., Payré, C., Mounier, C. M., Talvinen, K. A., Laine, V. J., Nevalainen, T. J., Gelb, M. H., and Lambeau, G. (2009) Group X phospholipase A_2 stimulates the proliferation of colon cancer cells by producing various lipid mediators. *Mol. Pharmacol.* **76,** 778–790
42. Neurath, M. F. (2014) Cytokines in inflammatory bowel disease. *Nat. Rev. Immunol.* **14,** 329–342
43. Saleh, M., and Elson, C. O. (2011) Experimental inflammatory bowel disease: insights into the host-microbiota dialog. *Immunity* **34,** 293–302
44. Logan, R. F. (1998) Inflammatory bowel disease incidence: up, down or unchanged? *Gut* **42,** 309–311
45. Morteau, O., Morham, S. G., Sellon, R., Dieleman, L. A., Langenbach, R., Smithies, O., and Sartor, R. B. (2000) Impaired mucosal defense to acute colonic injury in mice lacking cyclooxygenase-1 or cyclooxygenase-2. *J. Clin. Invest.* **105,** 469–478
46. Iizuka, Y., Okuno, T., Saeki, K., Uozaki, H., Okada, S., Misaka, T., Sato, T., Toh, H., Fukayama, M., Takeda, N., Kita, Y., Shimizu, T., Nakamura, M., and Yokomizo, T. (2010) Protective role of the leukotriene B_4 receptor BLT2 in murine inflammatory colitis. *FASEB J.* **24,** 4678–4690
47. Jia, Q., Lupton, J. R., Smith, R., Weeks, B. R., Callaway, E., Davidson, L. A., Kim, W., Fan, Y. Y., Yang, P., Newman, R. A., Kang, J. X., McMurray, D. N., and Chapkin, R. S. (2008) Reduced colitis-associated colon cancer in Fat-1 (*n*-3 fatty acid desaturase) transgenic mice. *Cancer Res.* **68,** 3985–3991
48. Bento, A. F., Claudino, R. F., Dutra, R. C., Marcon, R., and Calixto, J. B. (2011) ω-3 fatty acid-derived mediators 17(*R*)-hydroxy docosahexaenoic acid, aspirin-triggered resolvin D1 and resolvin D2 prevent experimental colitis in mice. *J. Immunol.* **187,** 1957–1969
49. Arita, M., Yoshida, M., Hong, S., Tjonahen, E., Glickman, J. N., Petasis, N. A., Blumberg, R. S., and Serhan, C. N. (2005) Resolvin E1, an endogenous lipid mediator derived from ω-3 eicosapentaenoic acid, protects against 2,4,6-trinitrobenzene sulfonic acid-induced colitis. *Proc. Natl. Acad. Sci. U.S.A.* **102,** 7671–7676
50. Elson, C. O., Sartor, R. B., Tennyson, G. S., and Riddell, R. H. (1995) Experimental models of inflammatory bowel disease. *Gastroenterology* **109,** 1344–1367

51. Oh, D. Y., Talukdar, S., Bae, E. J., Imamura, T., Morinaga, H., Fan, W., Li, P., Lu, W. J., Watkins, S. M., and Olefsky, J. M. (2010) GPR120 is an ω-3 fatty acid receptor mediating potent anti-inflammatory and insulin-sensitizing effects. *Cell* **142,** 687–698
52. Hara, S., Kamei, D., Sasaki, Y., Tanemoto, A., Nakatani, Y., and Murakami, M. (2010) Prostaglandin E synthases: understanding their pathophysiological roles through mouse genetic models. *Biochimie* **92,** 651–659
53. Kapoor, M., Kojima, F., Qian, M., Yang, L., and Crofford, L. J. (2006) Shunting of prostanoid biosynthesis in microsomal prostaglandin E synthase-1 null embryo fibroblasts: regulatory effects on inducible nitric oxide synthase expression and nitrite synthesis. *FASEB J.* **20,** 2387–2389
54. Escoffier, J., Jemel, I., Tanemoto, A., Taketomi, Y., Payre, C., Coatrieux, C., Sato, H., Yamamoto, K., Masuda, S., Pernet-Gallay, K., Pierre, V., Hara, S., Murakami, M., De Waard, M., Lambeau, G., and Arnoult, C. (2010) Group X phospholipase A_2 is released during sperm acrosome reaction and controls fertility outcome in mice. *J. Clin. Invest.* **120,** 1415–1428
55. Diep, Q. N., Touyz, R. M., and Schiffrin, E. L. (2000) Docosahexaenoic acid, a peroxisome proliferator-activated receptor-α ligand, induces apoptosis in vascular smooth muscle cells by stimulation of p38 mitogen-activated protein kinase. *Hypertension* **36,** 851–855
56. Ariyama, H., Kono, N., Matsuda, S., Inoue, T., and Arai, H. (2010) Decrease in membrane phospholipid unsaturation induces unfolded protein response. *J. Biol. Chem.* **285,** 22027–22035
57. Holzer, R. G., Park, E. J., Li, N., Tran, H., Chen, M., Choi, C., Solinas, G., and Karin, M. (2011) Saturated fatty acids induce c-Src clustering within membrane subdomains, leading to JNK activation. *Cell* **147,** 173–184
58. Dalli, J., Zhu, M., Vlasenko, N. A., Deng, B., Haeggström, J. Z., Petasis, N. A., and Serhan, C. N. (2013) The novel 13*S*,14*S*-epoxy-maresin is converted by human macrophages to maresin 1 (MaR1), inhibits leukotriene A_4 hydrolase (LTA4H), and shifts macrophage phenotype. *FASEB J.* **27,** 2573–2583
59. Titos, E., Rius, B., González-Périz, A., López-Vicario, C., Morán-Salvador, E., Martínez-Clemente, M., Arroyo, V., and Clària, J. (2011) Resolvin D1 and its precursor docosahexaenoic acid promote resolution of adipose tissue inflammation by eliciting macrophage polarization toward an M2-like phenotype. *J. Immunol.* **187,** 5408–5418
60. Kim, W., Khan, N. A., McMurray, D. N., Prior, I. A., Wang, N., and Chapkin, R. S. (2010) Regulatory activity of polyunsaturated fatty acids in T-cell signaling. *Prog. Lipid Res.* **49,** 250–261
61. Calviello, G., Palozza, P., Di Nicuolo, F., Maggiano, N., and Bartoli, G. M. (2000) *n*-3 PUFA dietary supplementation inhibits proliferation and store-operated calcium influx in thymoma cells growing in Balb/c mice. *J. Lipid Res.* **41,** 182–189
62. Ramon, S., Gao, F., Serhan, C. N., and Phipps, R. P. (2012) Specialized proresolving mediators enhance human B cell differentiation to antibody-secreting cells. *J. Immunol.* **189,** 1036–1042
63. Li, X., Shridas, P., Forrest, K., Bailey, W., and Webb, N. R. (2010) Group X secretory phospholipase A_2 negatively regulates adipogenesis in murine models. *FASEB J.* **24,** 4313–4324
64. Lai, Y., Oslund, R. C., Bollinger, J. G., Henderson, W. R., Jr., Santana, L. F., Altemeier, W. A., Gelb, M. H., and Hallstrand, T. S. (2010) Eosinophil cysteinyl leukotriene synthesis mediated by exogenous secreted phospholipase A_2 group X. *J. Biol. Chem.* **285,** 41491–41500
65. Kunisawa, J., Arita, M., Hayasaka, T., Harada, T., Iwamoto, R., Nagasawa R., Shikata, S., Nagatake, T., Suzuki, H., Hashimoto, E., Kurashima, Y., Suzuki, Y., Arai, H., Setou, M., and Kiyono, H. (2015) Dietary ω3 fatty acid exerts anti-allergic effect through the conversion to 17,18-epoxyeicosatetraenoic acid in the gut. *Sci. Rep.* **5,** 9750
66. Vijay, R., Hua, X., Meyerholz, D. K., Miki, Y., Yamamoto, K., Gelb, M., Murakami, M., and Perlman, S. (2015) Critical role of phospholipase A_2 group IID in age-related susceptibility to severe acute respiratory syndrome-CoV infection. *J. Exp. Med.* **212,** 1851–1868
67. Yamamoto, K., Miki, Y., Sato, M., Taketomi, Y., Nishito, Y., Taya, C., Muramatsu, K., Ikeda, K., Nakanishi, H., Taguchi, R., Kambe, N., Kabashima, K., Lambeau, G., Gelb, M. H., and Murakami, M. (2015) The role of group IIF-secreted phospholipase A_2 in epidermal homeostasis and hyperplasia. *J. Exp. Med.* **212,** 1901–1919
68. Masuda, S., Murakami, M., Matsumoto, S., Eguchi, N., Urade, Y., Lambeau, G., Gelb, M. H., Ishikawa, Y., Ishii, T., and Kudo, I. (2004) Localization of various secretory phospholipase A_2 enzymes in male reproductive organs. *Biochim. Biophys. Acta* **1686,** 61–76
69. Furimsky, A., Vuong, N., Xu, H., Kumarathasan, P., Xu, M., Weerachatyanukul, W., Bou Khalil, M., Kates, M., and Tanphaichitr, N. (2005) Percoll gradient-centrifuged capacitated mouse sperm have increased fertilizing ability and higher contents of sulfogalactosylglycerolipid and docosahexaenoic acid-containing phosphatidylcholine compared to washed capacitated mouse sperm. *Biol. Reprod.* **72,** 574–583
70. Lenzi, A., Gandini, L., Maresca, V., Rago, R., Sgrò, P., Dondero, F., and Picardo, M. (2000) Fatty acid composition of spermatozoa and immature germ cells. *Mol. Hum. Reprod.* **6,** 226–231
71. Dalli, J., Chiang, N., and Serhan, C. N. (2015) Elucidation of novel 13-series resolvins that increase with atorvastatin and clear infections. *Nat. Med.* **21,** 1071–1075
72. Kaur, G., Cameron-Smith, D., Garg, M., and Sinclair, A. J. (2011) Docosapentaenoic acid (22:5*n*-3): a review of its biological effects. *Prog. Lipid Res.* **50,** 28–34